Supporting Information

Dehydrogenation of Iron Amido-Borane and Resaturation of the Imino-Borane Complex

Xiaofang Zhai,[‡] Maofu Pang, Lei Feng, Jiong Jia, Chen-Ho Tung and Wenguang Wang*

School of Chemistry and Chemical Engineering, Shandong University, 27 South Shanda Road, Jinan, 250100, China. Email: wwg@sdu.edu.cn

Table of contents

1. General information

All reactions were performed in flame-dried glassware using standard Schlenk techniques or in a glovebox under nitrogen atmosphere. Hexane, THF, diethyl ether and acetonitrile were dried and degassed by Solvent Purification Systems (Innovative Technology). C_6H_6 and C_6D_6 was dried with 4Å molecular sieves and degassed by freeze-pump-thaw method. Fluorobenzene was dried over P_2O_5 for two days under nitrogen and degassed by freeze-pump-thaw method. Pentane was dried over sodium for two days and degassed by freeze-pump-thaw method. All reagents were purchased from Sigma-Aldrich and used without further purification unless otherwise noted. The 1,2-(diphenylphosphino)benzeneamine (1,2-$Ph_2PC_6H_4NH_2$)[1] and [Cp*Fe(NCMe)$_3$]PF_6[2] were prepared according to reported procedures. NMR spectra were recorded on Bruker 500 (500 MHz for ^{1}H, 126 MHz for ^{13}C, 202 MHz for ^{31}P, 160 MHz for ^{11}B) spectrometers. Chemical shifts for ^{1}H spectra were referenced to residual solvent resonances. $BF_3{\cdot}OEt_2$ was used as external standard for ^{11}B NMR, and ^{31}P NMR chemical shifts are referenced to external H_3PO_4. The chemical shifts are reported in ppm relative to either the residual solvent peak or TMS as an internal standard. Coupling constants (*J*) were reported in Hz. Attribution of peaks were performed based on the multiplicities and integrals of the peaks.

Single crystals with appropriate dimensions were selected under an optical microscope and quickly coated with high vacuum grease (Dow Corning Corporation) to prevent decomposition. Crystallographic data were collected using a Bruker D8 VENTURE with Mo Kα radiation (λ = 0.71073 Å) and micro-focus Cu Kα radiation (λ = 1.5418 Å) at 173 K. Crystal data collection and refinement parameters are summarized in Tables S2-S3.

MS (HRMS) measured with ThermoFisher Q-Exactive Mass Spectrometer. Elemental analyses (C, and H) were performed on Elementar Vario EL III analyzer, and samples were handled under N_2 atmosphere wherever appropriate.

2. Experimental procedures

2.1 Synthesis of Cp*Fe(BH$_4$)NCMe (1)

The limited stability of complex **1** prevented its isolation. Bu$_4$NBH$_4$ (103 mg, 0.4 mmol) in 5 mL CH$_3$CN was added to the solution of [Cp*Fe(NCMe)$_3$]PF$_6$ (200 mg, 0.4 mmol) in 30 mL CH$_3$CN, the color turned from purple to dark blue immediately. After stirring for 5 min at room temperature, the solution was layed with diethyl ether and was stored at -30 ^{o}C for several days to afford **1** (75 mg, yield 75%) as dark blue crystals. ^{11}B {1H} NMR (160 MHz, CD$_3$CN): δ 15.4 (quintet, J_{BH} = 88 Hz).

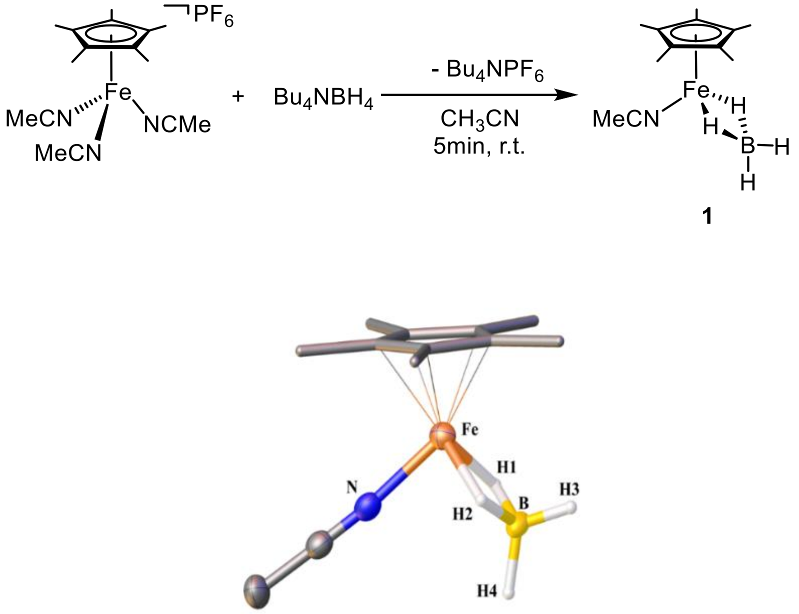

Figure S1. Synthetic route to Cp*Fe(BH$_4$)NCMe (**1**) and its solid-state structure of with 50% probability thermal ellipsoids. For clarity, some hydrogen atoms are omitted. Selected bond distances (Å) and angles (deg): Fe-N, 1.908(3); Fe-H1, 1.64(3); Fe-H2, 1.66(4); Fe-B, 2.104(4); B-H1, 1.25(3); B-H2, 1.26(4); B-H3, 1.10(4); B-H4, 1.16(5); H1-Fe-H2, 73.407 ^{o}.

2.2 Synthesis of Cp*Fe(η^1-H$_3$B-NHC$_6$H$_4$Ph$_2$P) (2)

In a 100 mL Schlenk flask, Bu$_4$NBH$_4$ (103 mg, 0.4 mmol) in 5 mL CH$_3$CN was added to the solution of [Cp*Fe(NCMe)$_3$]PF$_6$ (200 mg, 0.4 mmol) in 30 mL CH$_3$CN, the color turned from purple to dark blue immediately. After stirring for 10 min at room temperature, 1,2-Ph$_2$PC$_6$H$_4$NH$_2$ (110.8 mg, 0.4 mmol) in 5 ml CH$_3$CN was added to the reaction mixture, the solution turned to dark brown and kept stirring for 1 h. The solvent was pumped off and residue was extracted with hexane (20 mL). The resulting hexane solution was concentrated and cooled at -30 ℃ for a few days to give Cp*Fe(1,2-$Ph_2PC_6H_4NH$)(η^1–BH_3) (**2**) (167 mg, yield 87%) as brown solid. Anal. Calcd for $C_{28}H_{33}FeBPN$: C, 69.89; H, 6.91. Found: C, 69.75; H, 6.87. ESI-MS calcd. 481.1793; found, 481.1770. ^{1}H NMR (500 MHz, C_6D_6): δ 8.18 (t, *J* = 10.0 Hz, 2H, Ar*H*), 7.22-7.25 (m, 3H, Ar*H*), 7.12-7.16 (m, 2H, Ar*H*), 7.06-7.09 (m, 1H, Ar*H*), 6.98-7.03 (m, *J* = 3H, Ar*H*), 6.86-6.89 (m, 1H, Ar*H*), 6.82 (t, *J* = 10 Hz, 1H, Ar*H*), 6.68 (t, *J* = 7.5 Hz, 1H, Ar*H*), 2.73(s, 1H, N*H*), 2.22 (br, 1H, B*H*), 1.54 (s, 15H, $CpMe_5$), 0.12 (br, 1H, B*H*), -13.98 (s, 1H, Fe-*H*-B);^{13}C NMR (126 MHz, C_6D_6) δ 166.38 (d, *J* = 25.2 Hz), 139.63 (s), 139.33 (s), 136.47 (s), 134.54 (d, *J* = 12.6 Hz), 133.86 (d, *J* = 10.08 Hz), 133.59 (d, *J* = 10.08 Hz), 133.16 (s), 132.90 (s), 132.40 (s), 131.20 (s), 129.66 (s), 129.30 (s), 128.89 (s), 123.48 (d, *J* = 5.04 Hz), 120.36 (d, *J* = 8.82 Hz), 81.24 (s), 10.48 (s); ^{31}P {1H} NMR (202 MHz, C_6D_6): δ 85.9 (s); ^{11}B NMR (160 MHz, C_6D_6): δ -17.5 (s).

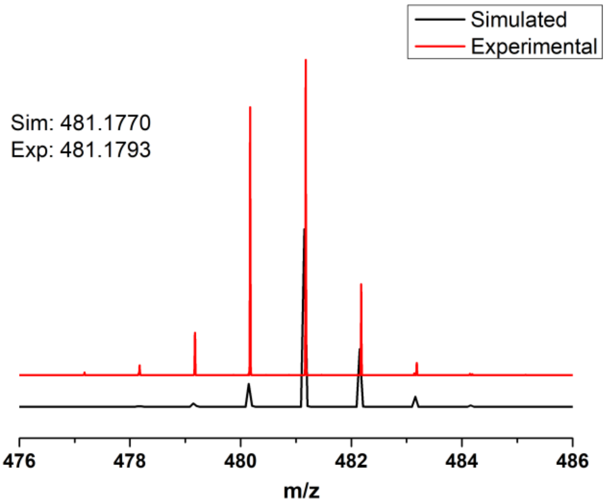

Figure S2. ESI-MS spectrum of Cp*Fe(η^1-H_3B-$NHC_6H_4Ph_2P$) (**2**) (80 V, 200 ^{0}C, hexane)

2.3 Synthesis of Cp*Fe(η^2-H_2B=$NHC_6H_4Ph_2P$) (3).

In a 50 mL Schlenk flask, a solution of **2** (150 mg, 0.3 mmol) in 10 mL benzene was heated to 50 ^{o}C for 6 hours. Then the solvent was pumped off and the reaction residue was extracted by hexane (10 mL). Hexane was removed *in vacuo* to give complex **3** as reddish brown solid (137 mg, 92% yield). Crystals suitable for X-ray analysis were obtained from concentrated hexane solution of **3** at -30 °C. Anal. Calcd for $C_{28}H_{31}FeBPN$: C, 70.18; H, 6.52. Found: C, 70.23; H, 6.58. ESI-MS calcd. 479.1637; found, 479.1626. ^{1}H NMR (500 MHz, C_6D_6): δ 7.80 (m, 4H, Ar*H*), 7.31 (t, *J* = 10 Hz, 1H, Ar*H*), 7.10 (td, *J* = 5.0 Hz, 7.5 Hz, 4H, Ar*H*), 7.01-7.04 (m, 2H, Ar*H*), 6.82 (t, *J* = 10 Hz, 1H, Ar*H*), 6.55 (t, *J* = 10 Hz, 1H, Ar*H*), 6.04 (t, *J* = 1H, Ar*H*), 1.56 (s, 15H, CpMe$_5$), -17.93 (s, 2H, Fe-*H*-B); ^{13}C NMR (126 MHz, C_6D_6) δ 151.48 (d, *J* = 12.6 Hz), 140.45 (s), 140.17 (s), 134.47 (s), 134.40 (s), 134.31 (s), 130.15 (s), 128.64 (s), 119.76 (d, *J* = 7.56 Hz), 118.89 (d, *J* = 5.04 Hz), 112.69 (s), 112.40 (s); 85.41 (s), 10.67 (s); ^{31}P {1H} NMR (202 MHz, C_6D_6): δ 71.9(s); ^{11}B NMR (160 MHz, C_6D_6): δ 42.7 (s).

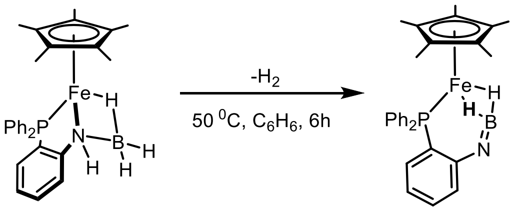

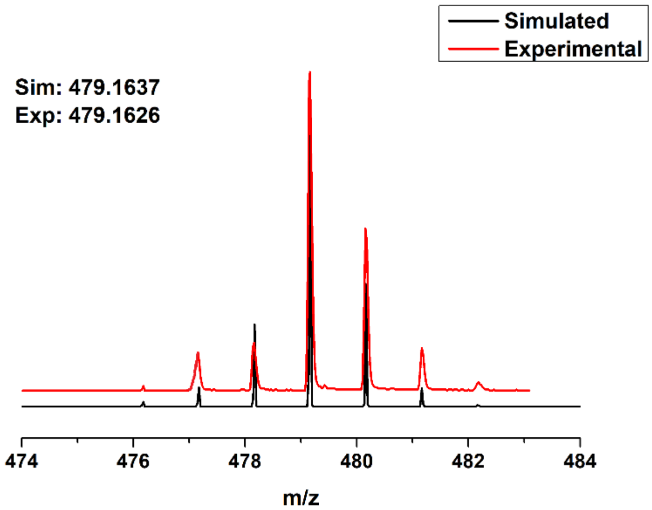

Figure S3. ESI-MS spectrum of Cp*Fe(η^1-$H_2B{=}NHC_6H_4Ph_2P$) (**3**) (80 V, 200 ^{0}C, hexane).

Quantification of H_2 by GC-TCD

H_2 was identified by a Techcomp7890 II gas chromatograph (GC) equipped with a 5 Å molecular sieve column using argon as carrier gas and a thermal conductivity detector (TCD). Under argon, 3 mL benzene solution of **2** (30 mg, 0.06 mmol) was placed into a 10 mL reaction tube with a rubber plug. The flask was sealed by wax and was immersed in a 50 °C bath for 6 h. The volume of the evolved hydrogen was monitored by GC-TCD with methane (1.00 mL) as the internal standard. Three parallel reactions were conducted and 1.31, 1.29, and 1.36 mL H_2 (Calcd 1.34 mL) was detected, respectively. The ^{31}P NMR spectrum of the reaction confirmed the formation of complex **3**.

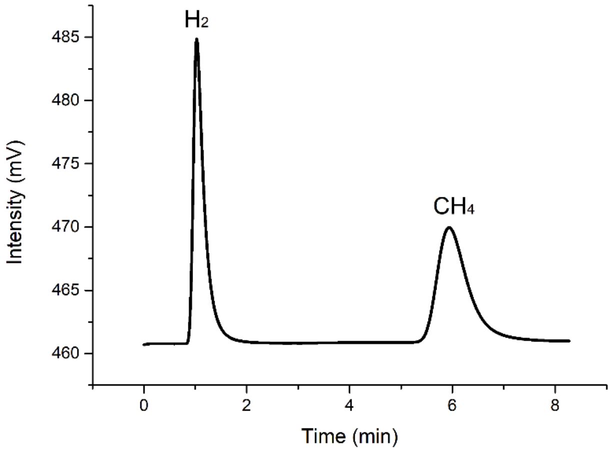

Figure S4. A representative GC-TCD profile for the quantification of H_2 generated in the dehydrogenation reaction of **2** to form **3**.

2.4 Synthesis of Cp*Fe(η^1-D_3B-$NHC_6H_4PPh_2$) (*d*-2) and Cp*Fe(η^2-D_2B=$NHC_6H_4PPh_2$) (*d*-3)

Cp*Fe(η^1-D_3B-$NHC_6H_4PPh_2$) (*d*-2). In a 100 mL Schlenk flask, $NaBD_4$ (20 mg, 0.48 mmol) was added to the solution of $[Cp^*Fe(NCMe)_3]PF_6$ (200 mg, 0.4 mmol) in 30 mL CH_3CN. The reaction was stired for 1h before 1,2-$Ph_2PC_6H_4NH_2$ (110.8 mg, 0.4 mmol) in 5 ml CH_3CN was added. The reaction flask was immersed in a 35 °C bath and kept stirring for 2 h. The solvent was pumped off and the residue was extracted by hexane. Dark brown solid was obtained after the removal of residue solvent (132 mg, 68% yield). The solid was recystallized from hexane at -20 °C. ^2H NMR (77 MHz, C_6H_6), δ 2.23 (s, B-*D*), 0.19 (s, B-*D*), -13.98 (s, Fe-*D*-B). ESI-MS calcd. 484.1987; found, 484.1976.

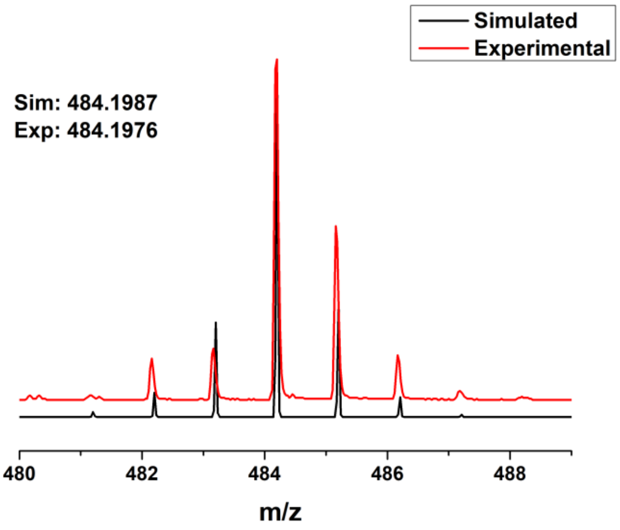

Figure S5. ESI-MS spectrum of Cp*Fe(η^1-D_3B-NHC$_6$H$_4$PPh$_2$) (***d*-2**). (80 V, 200 ^{0}C, hexane).

Cp*Fe(η^2-D_2B=NHC$_6$H$_4$PPh$_2$) (*d*-3). In a 50 mL Schlenk flask, a solution of ***d*-2** (100 mg, 0.2 mmol) in 10 mL benzene was heated to 50 ºC for 6 hours. Then the solvent was pumped off and the reaction residue was extracted by hexane (10 mL). Hexane was removed *in vacuo* to give complex ***d*-3** as reddish brown solid (76 mg, 80% yield). The solid was recystallized from hexane at -20 ºC. ^{2}H NMR (77 MHz, C$_6$H$_6$), δ -17.94 (s, Fe-*D*-B). ESI-MS calcd. 481.1768; found, 484.1753.

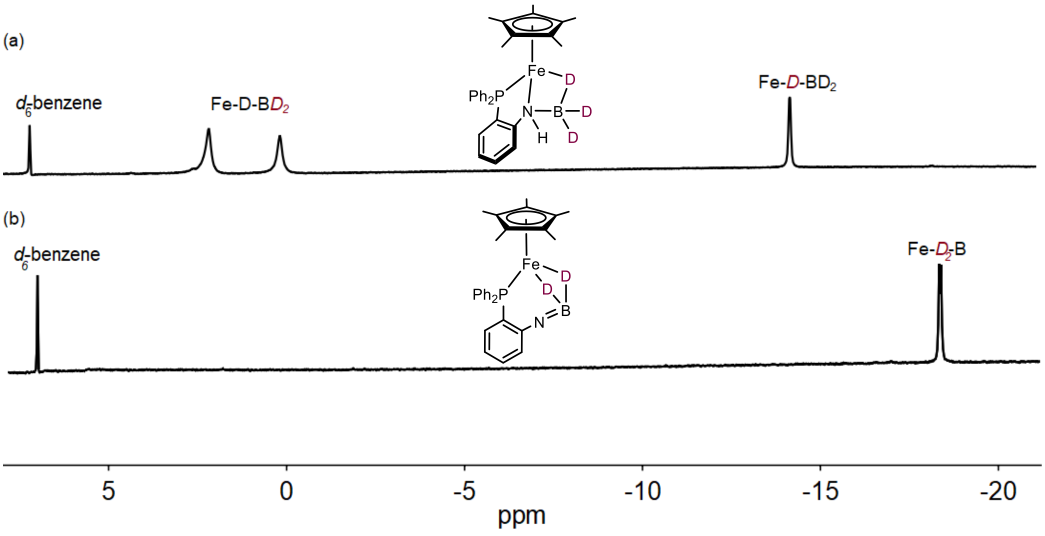

Figure S6. (a) ^{2}H NMR spectrum of ***d*-2** in C$_6$H$_6$; (b) ^{2}H NMR spectrum of ***d*-3** in C$_6$H$_6$.

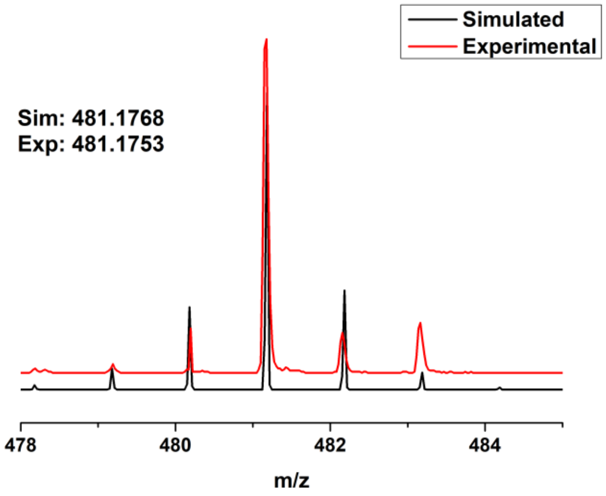

Figure S7. ESI-MS spectrum of Cp*Fe(η^2-D_2B=$NHC_6H_4PPh_2$) (***d*-3**). (80 V, 200 ^{0}C, hexane).

3. NMR spectra of the synthesized Fe complexes

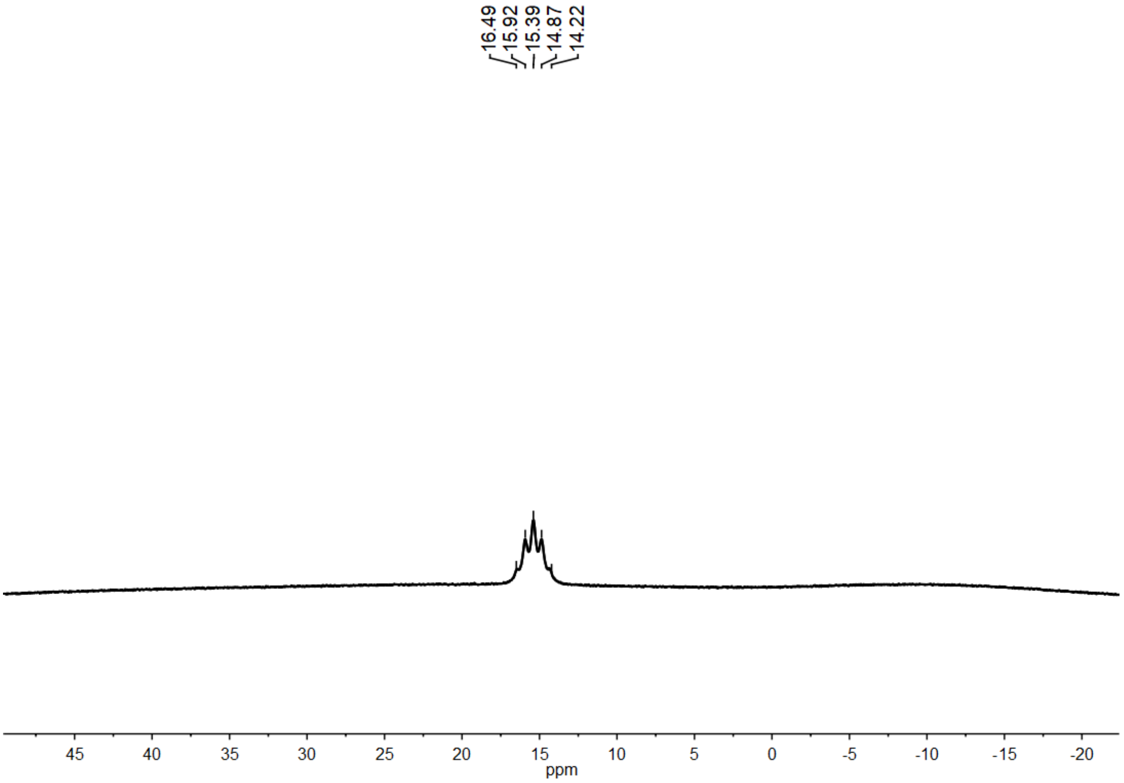

Figure S8. ^{11}B NMR spectrum of **1** in CD_3CN.

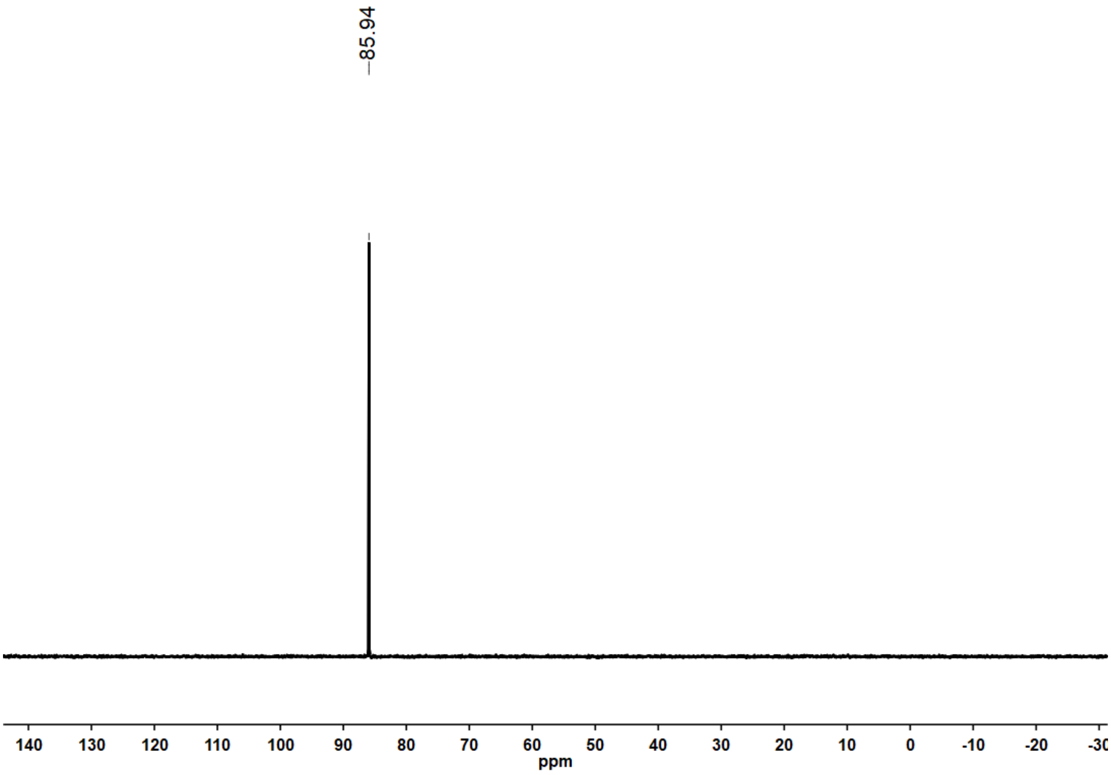

Figure S9. ^{31}P NMR spectrum of **2** in C_6D_6.

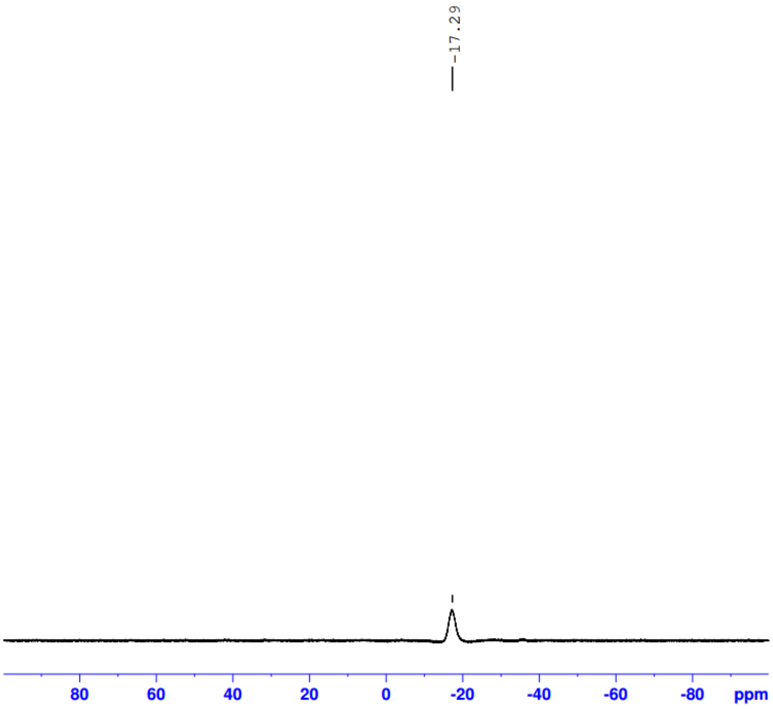

Figure S10. ^{11}B NMR spectrum of **2** in C_6D_6.

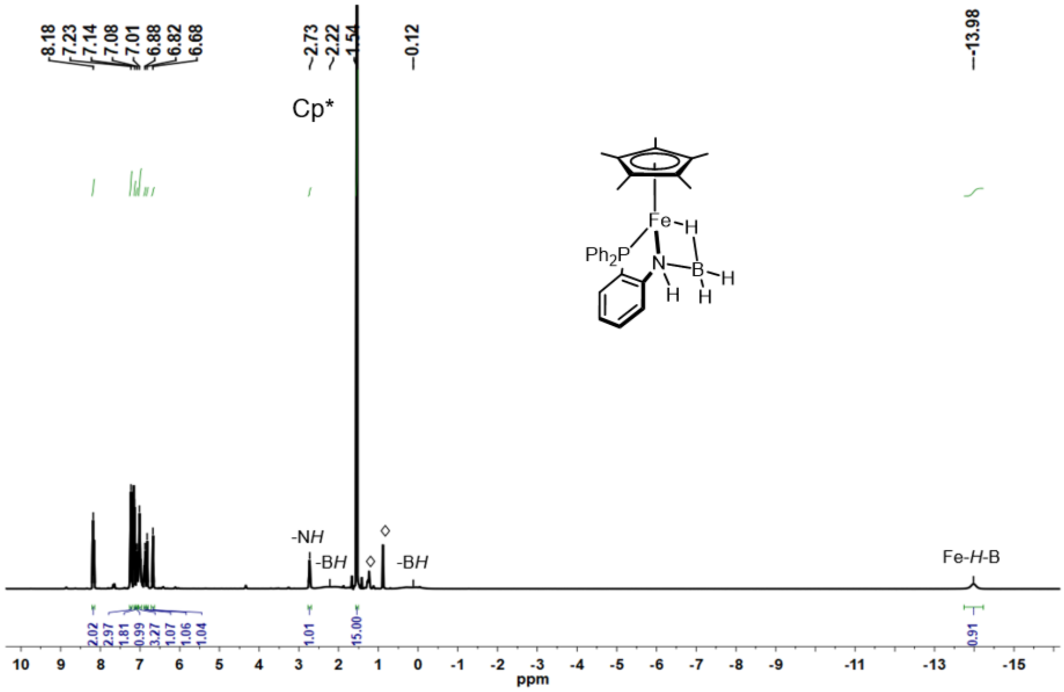

Figure S11. ^{1}H NMR spectrum of **2** in C_6D_6. (◇solvent residue)

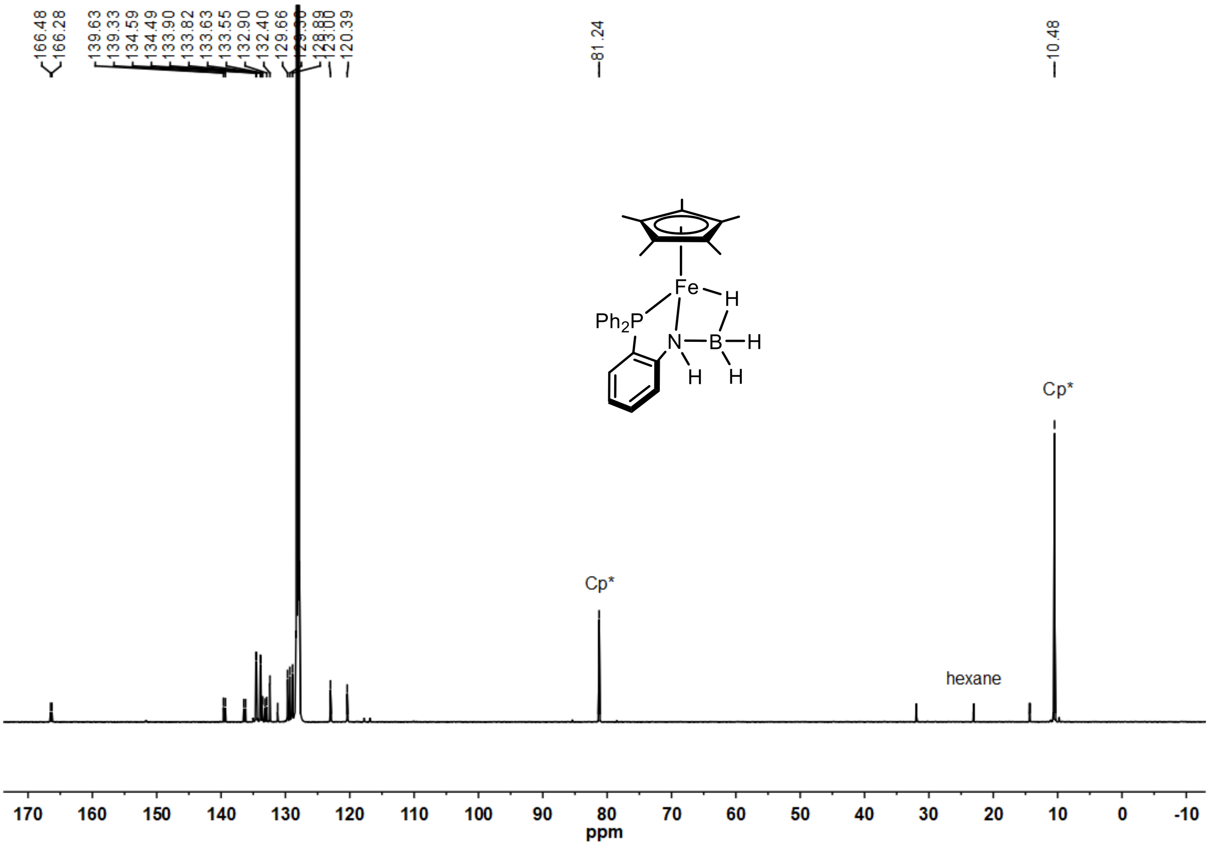

Figure S12. ^{13}C NMR spectrum of **2** in C_6D_6.

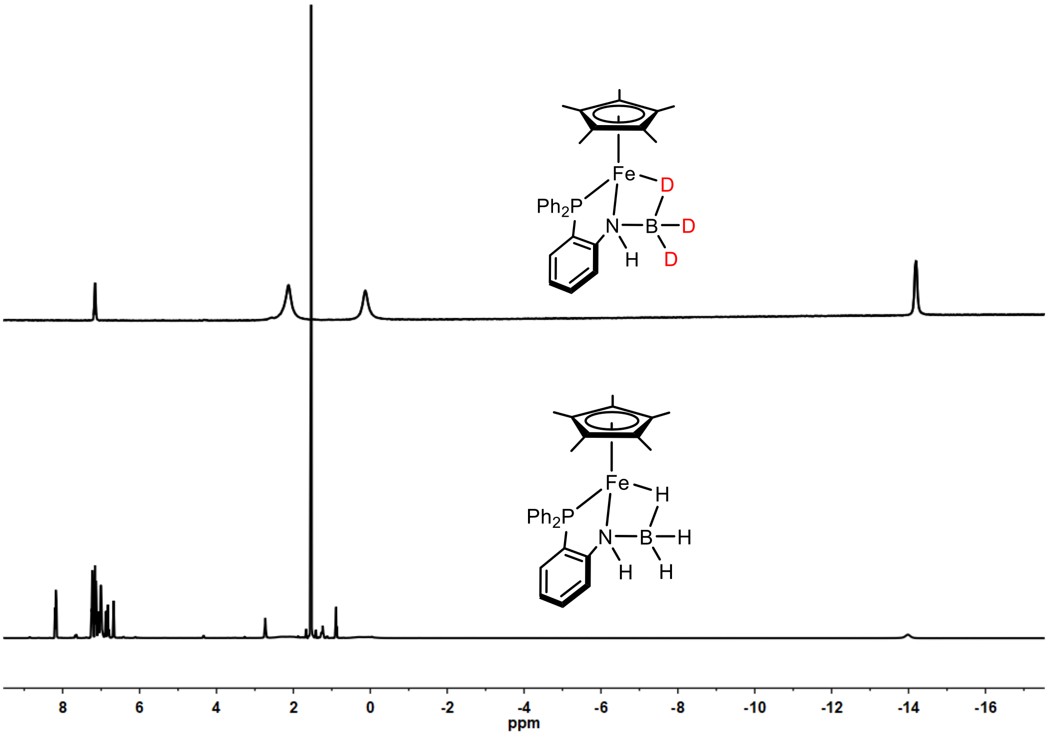

Figure S13. Top: ^{2}H NMR spectrum of **2** (C_6H_6); Bottom: ^{1}H NMR spectrum of **2** (C_6D_6).

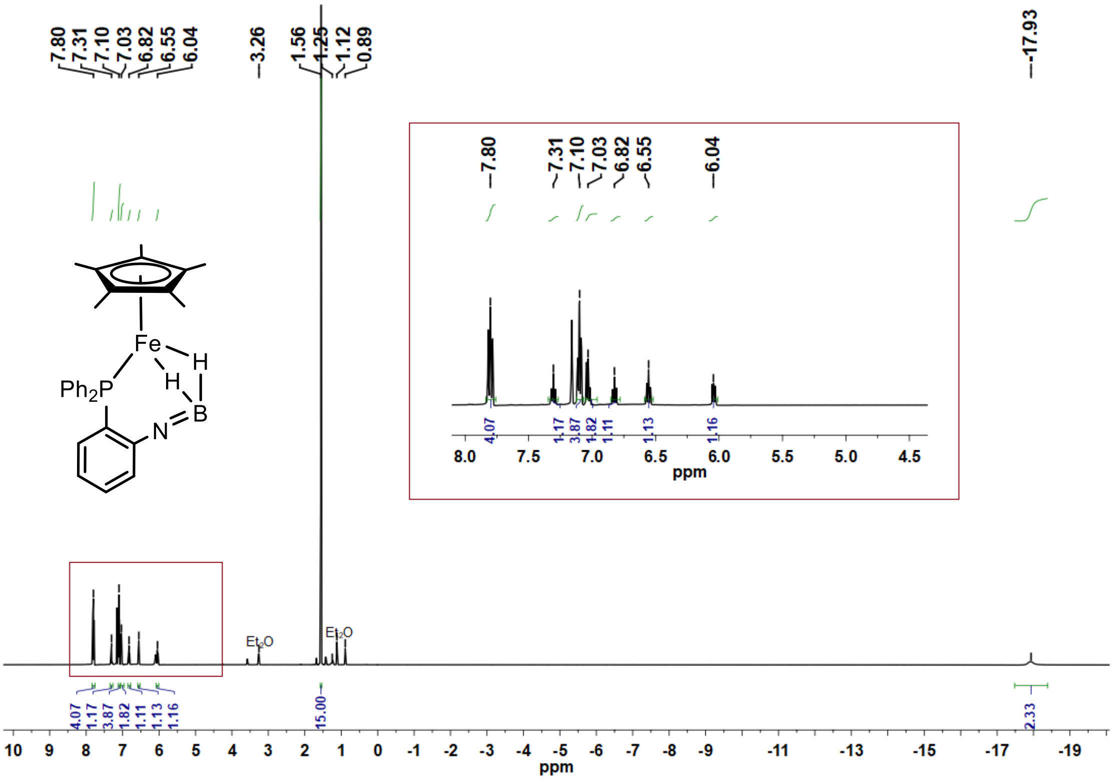

Figure S14. ^{1}H NMR spectrum of **3** in C_6D_6.

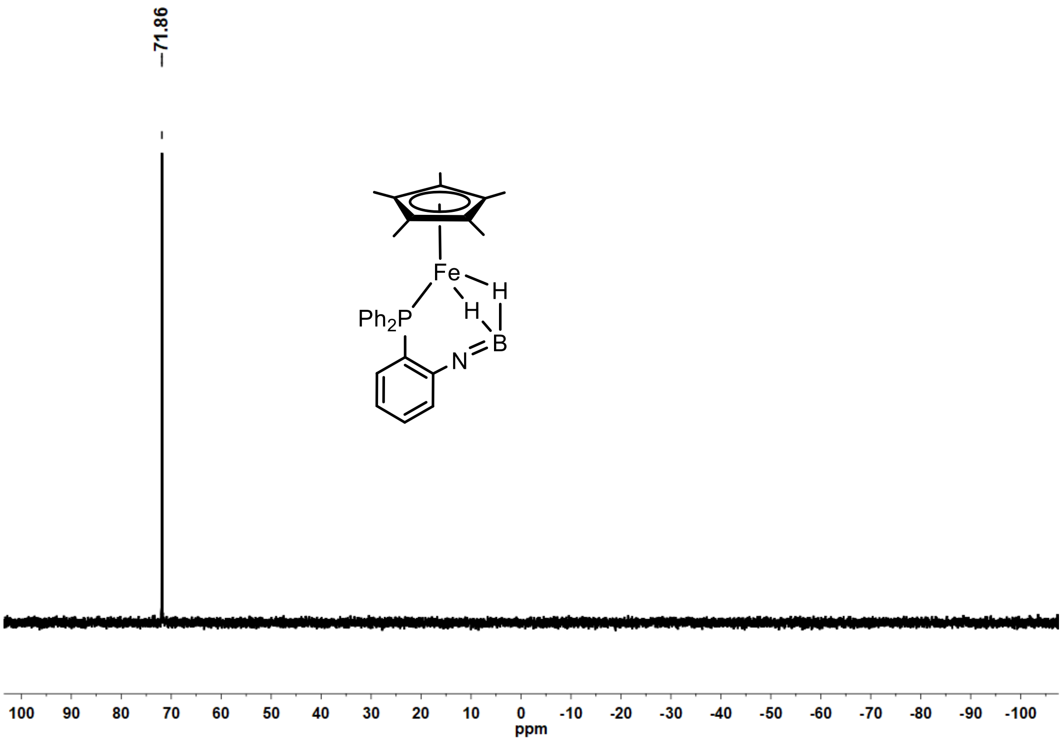

Figure S15. ^{31}P NMR spectrum of **3** in C_6D_6.

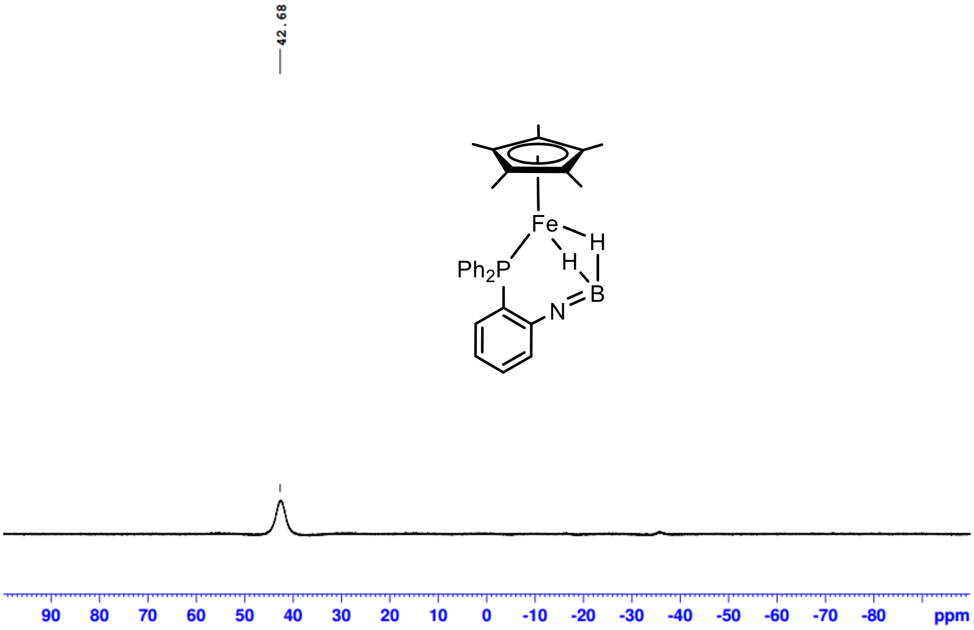

Figure S16. ^{11}B NMR spectrum of **3** in C_6D_6.

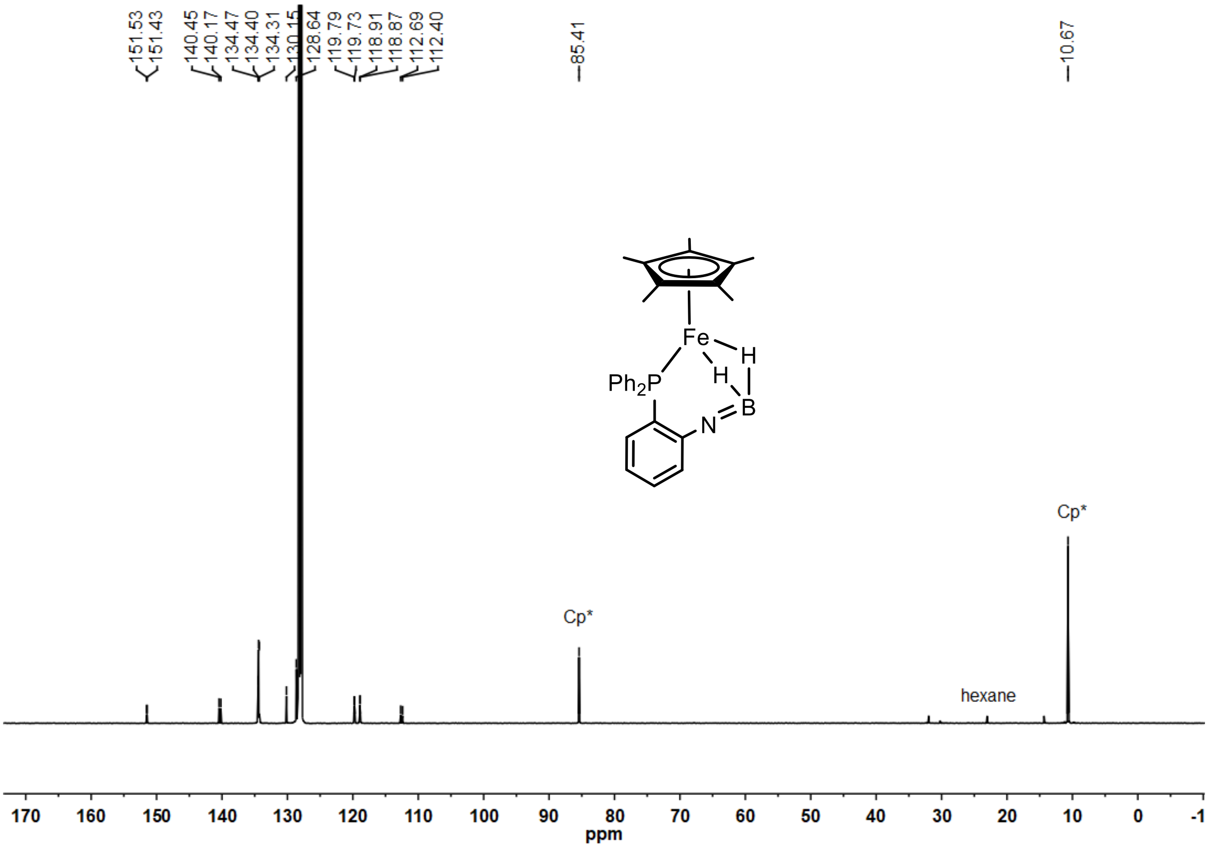

Figure S17. ^{13}C NMR spectrum of **3** in C_6D_6.

4. Dehydrogenation of *d*-2.

In glovebox, *d*-**2** (20 mg, 0.04 mmol) was dissolved in 0.6 ml C_6D_6 and the solution was transfer to a J-Young NMR tube which was then sealed and immersed in a 50 ºC bath for 4 h. The J-Young tube was cooled to 10 ºC for 1 h and shaked several times before ^{1}H NMR spectrum was collected.

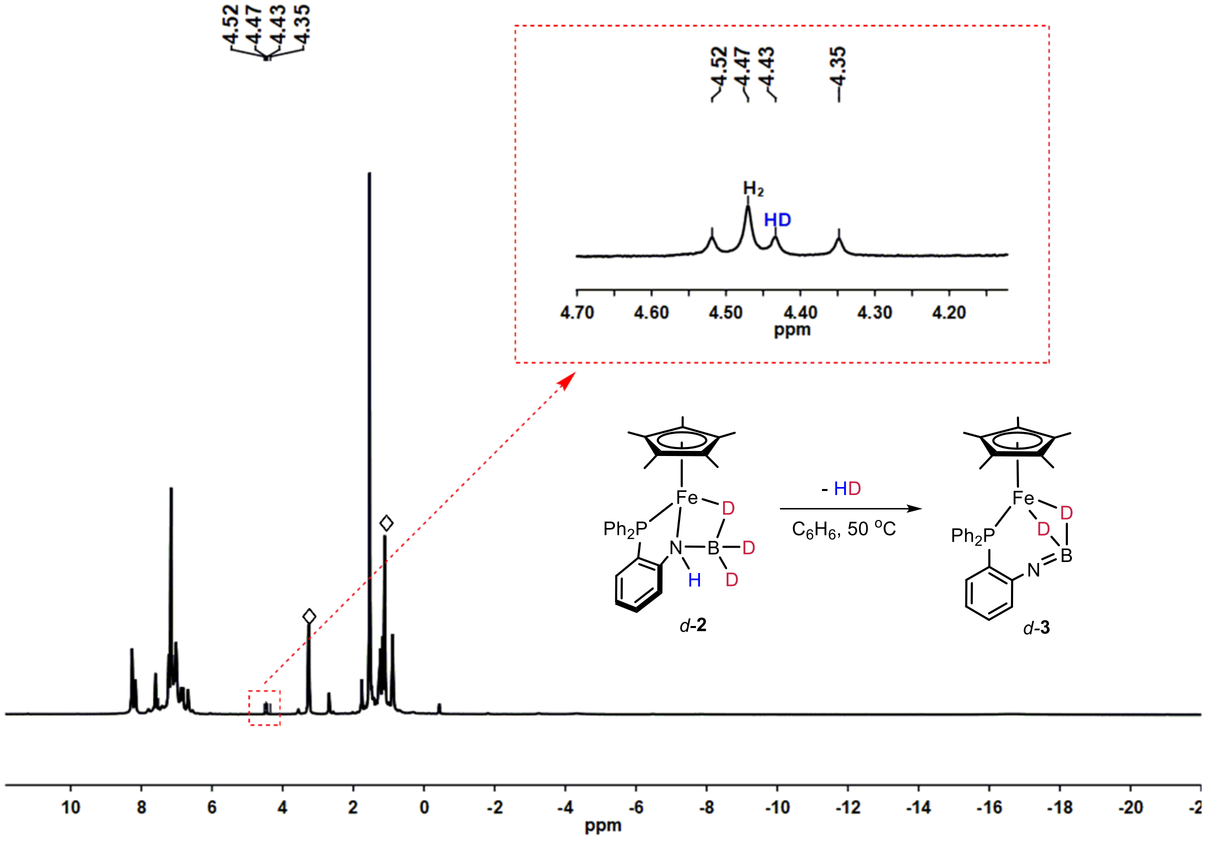

Figure S18. ^{1}H NMR spectrum (C_6D_6) for the dehydrogenation reaction of *d*-**2** (◇ solvent residue).

5. Protonation of complex 3 with $H(Et_2O)_2BAr_4^F$

In a glovebox, a 10 ml glass vial containing a stir bar was charged with complex **3** (20 mg, 0.04 mmol) in 2 mL fluorobenzene. $H(Et_2O)_2BAr_4^F$(40.5 mg, 0.04 mmol) in 2 mL fluobenzene was added dropwise. The reaction was stirred for 0.5 h and the solvent was removed under reduced pressure. The residue was washed with hexane (5 mL × 3) and dried under vaccum to give [**3H**][BAr_4^F] as black solid (48 mg, 91% yield). Crystals suitable for X-ray analysis were obtained by layering hexane to a concentrated solution of [**3H**][BAr_4^F] in diethyl ether at -30 °C.

Alternatively, [**3H**][BAr_4^F] can be produced via the reaction of complex **2** with $H(Et_2O)_2BAr_4^F$. Complex **2** (20 mg, 0.04 mmol) was dissolved in 2 mL fluorobenzene and subsequently $H(Et_2O)_2BAr_4^F$(40.5 mg, 0.04 mmol) was added, upon which hydrogen bubbles formed immediately. The amount of H_2 generated was monitored by GC-TCD with methane

(1.00 mL) as the internal standard. Three parallel reactions were conducted and 0.84, 0.87, and 0.85 mL H_2 (Calcd 0.896 mL) was detected, respectively. The reaction was stired for 0.5 h before the solvent was removed. The residue was washed with hexane (5 mL × 3) and dried under vaccum. ESI-MS calcd. 480.1715; found, 480.1726.

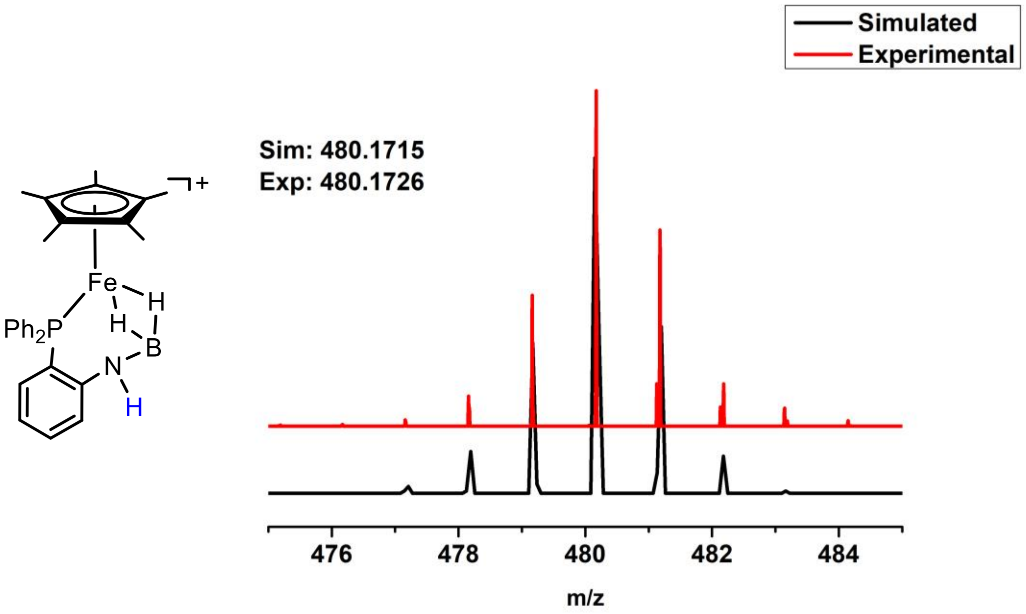

Figure S19. ESI-MS spectrum of [**3H**][BAr_4^F] (80 V, 100 °C, Et_2O).

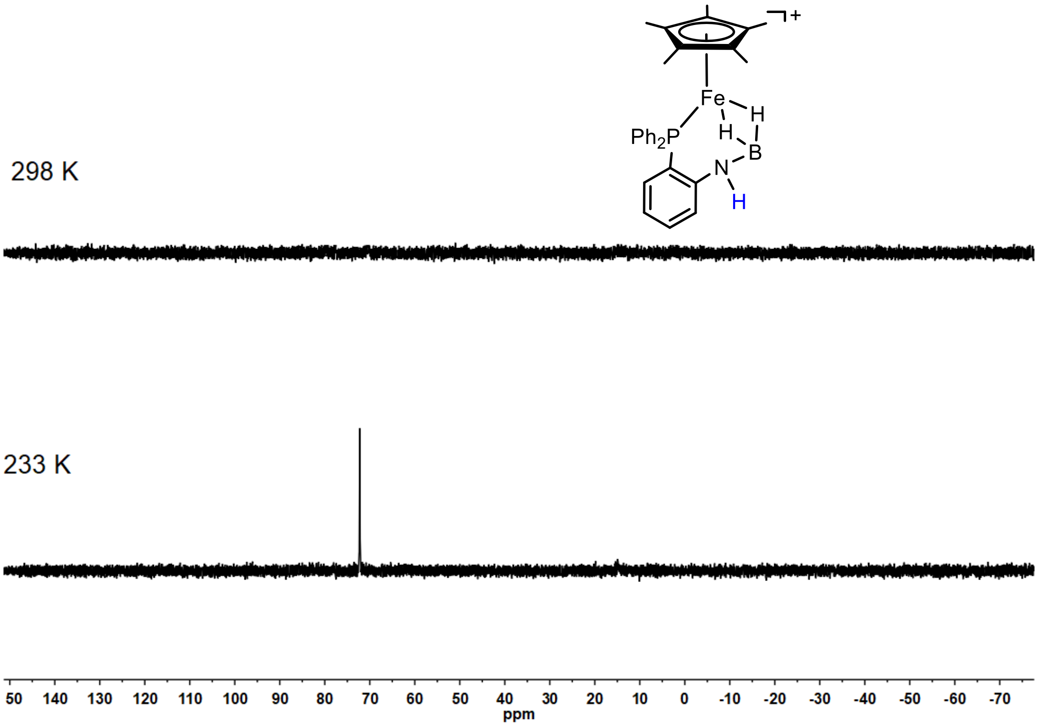

Figure S20. Low-temperature ^{31}P NMR spectrum of [**3H**][BAr_4^F] in d_8-THF.

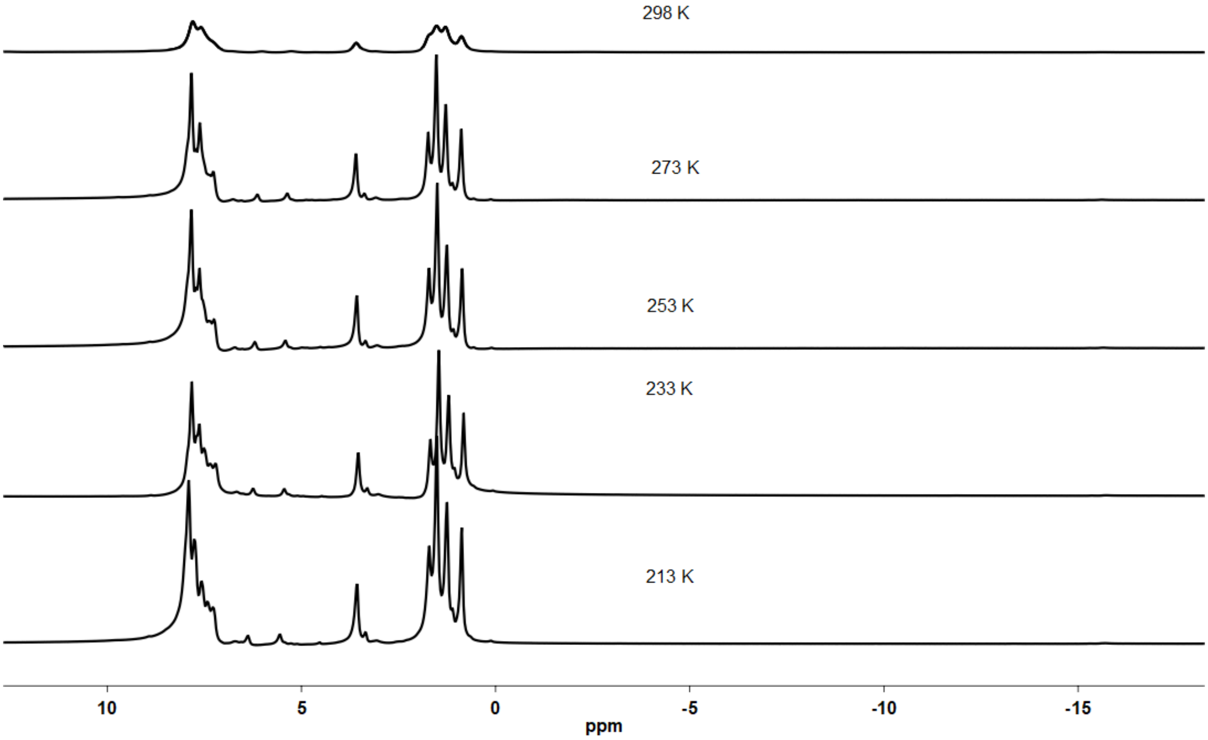

Figure S21. Low-temperature ^{1}H NMR spectrum of [**3H**][BAr$_4^F$] in *d*$_8$-THF.

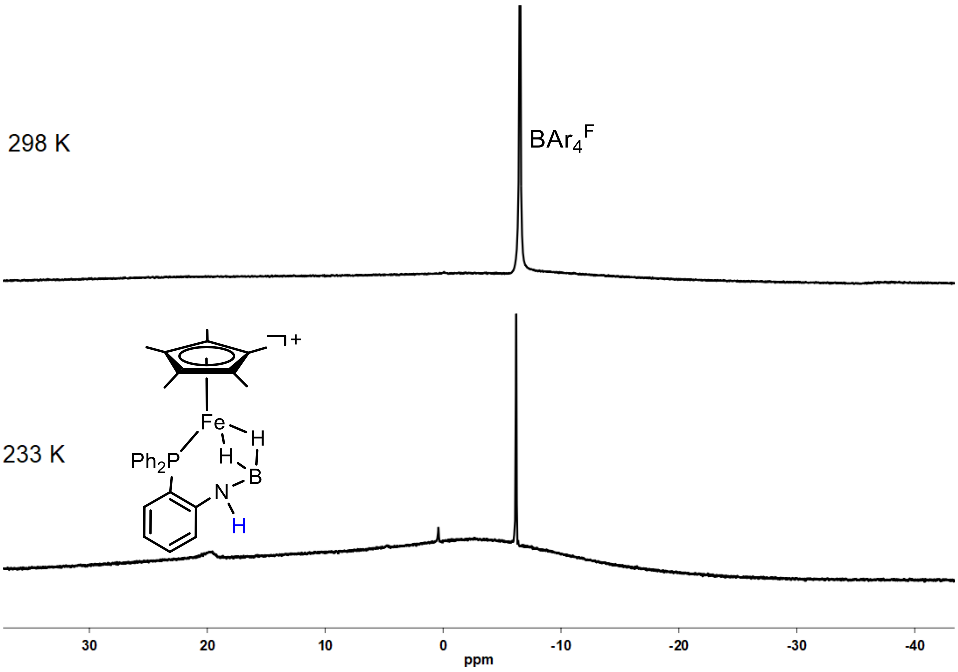

Figure S22. Low-temperature ^{11}B NMR spectrum of [**3H**][BAr$_4^F$] in *d*$_8$-THF.

The magnetic moment of [**3**H]$^+$ was determined to be 0 by Evans method. Tetramethylsilane (TMS) was used for the measurement. The solution without analyte was prepared in sealed capillary with 0.1 mL of a 99.8% of CDCl3 and TMS (v/v = 99:1). ^{1}H NMR (500 MHz) was recorded at 25 °C for [3H]$^+$. No frequency shift was observed for TMS signal with respect to [**3H**]$^+$.

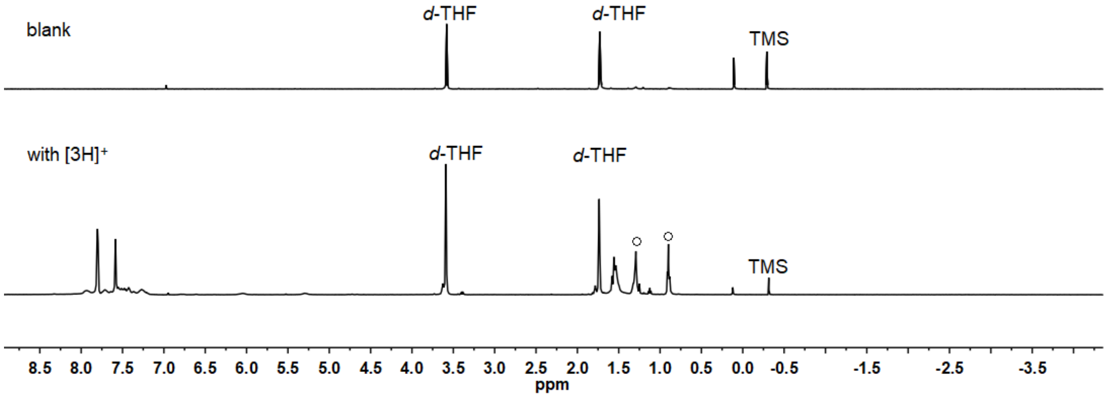

Figure S23. ^{1}H NMR spectra for the measurement of magnetic moment. (○ hexane residue)

6. Reaction of 2 or 3 with [HPPh$_3$][BAr$_4^F$]

Synthesis of [HPPh$_3$][BAr$_4^F$]. Under nitrogen, H(Et$_2$O)$_2$(BAr$_4^F$) (300 mg, 0.3 mmol) was dissolved in 15 mL diethyl ether in a 50 mL Schlenk flask. PPh$_3$ (78 mg, 0.3 mmol) was then added to the solution and the solution stirred for 0.5 h. The solvent was removed under vacuum to afford the product as white solid (324 mg, 96% yield).

[**3H**(**PPh$_3$**)][BAr$_4^F$] was prepeared in a similar manner to [**3H**][BAr$_4^F$]. In a 10 mL vial complex **2** or **3** (20 mg, 0.04 mmol) was dissolved in 2 mL fluorobenzene, to which a solution of [HPPh$_3$][BAr$_4^F$] (45 mg, 0.04 mmol) was added. After stirring for 0.5 h, the reaction solution was concentrated and 8 mL pentane was layred. The vial was stored for 3 days at -30 °C to afford crystals suitable for X-ray diffraction. Inspite of extensive efforts, we could not obtain a very clean ^{1}H NMR spectrum of [**3H**(**PPh$_3$**)][BAr$_4^F$] even after multiple recrystallization because the PPh$_3$-BH$_2$-NHAr moity prones to decoordinate from iron even at low temperatures.[3] ESI-MS calcd. 742.2626; found, 742.2620. ^{1}H NMR (500 MHz, *d$_8$*-THF): δ 4.68 (s, N*H*), 1.55 (s, 15H, CpMe$_5$), -15.58 (Fe-*H*-B), in situ ^{31}P{1H} NMR (202 MHz, C$_6$H$_5$F): δ 78.9 (s), -1.3 (s); ^{11}B NMR (160 MHz, C$_6$H$_5$F): δ -6.0 (s), -13.7 (s).

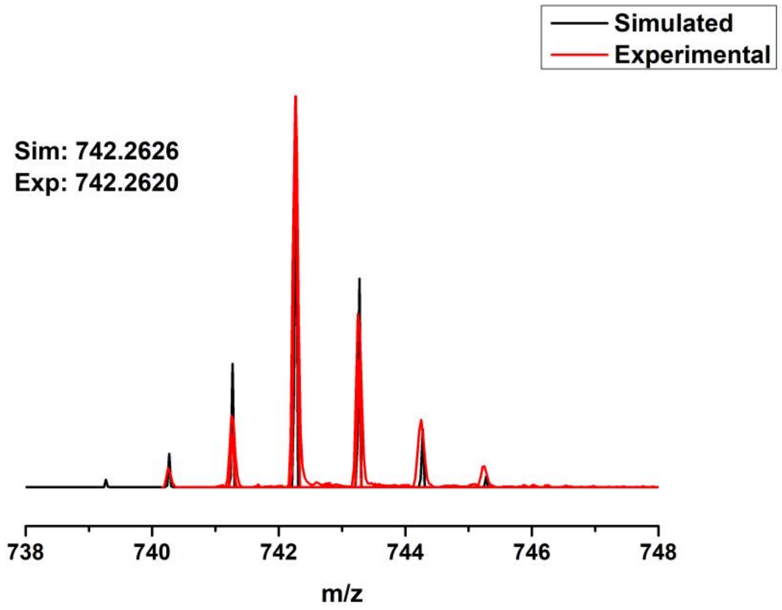

Figure S24. ESI-MS spectrum of [**3H(PPh$_3$)**][BAr$_4$^{F}] (80 V, 100 ºC, Et$_2$O).

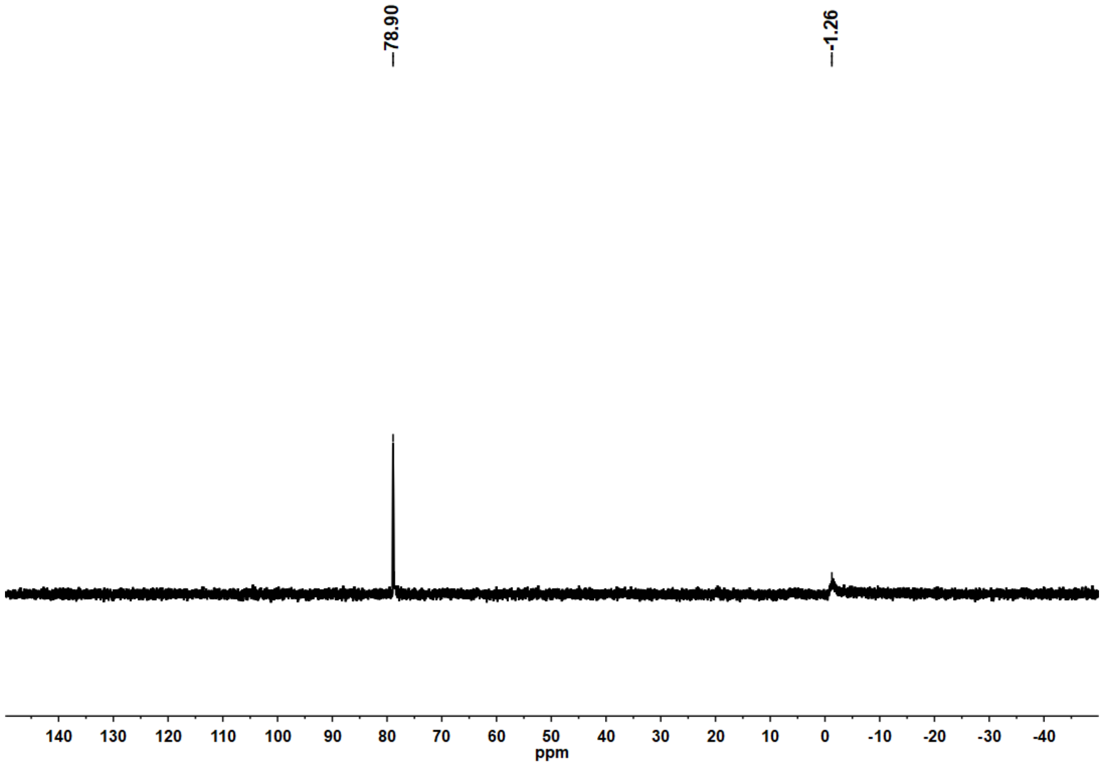

Figure S25. ^{31}P NMR spectrum of [**3H(PPh$_3$)**][BAr$_4$^{F}] in fluorobenzene.

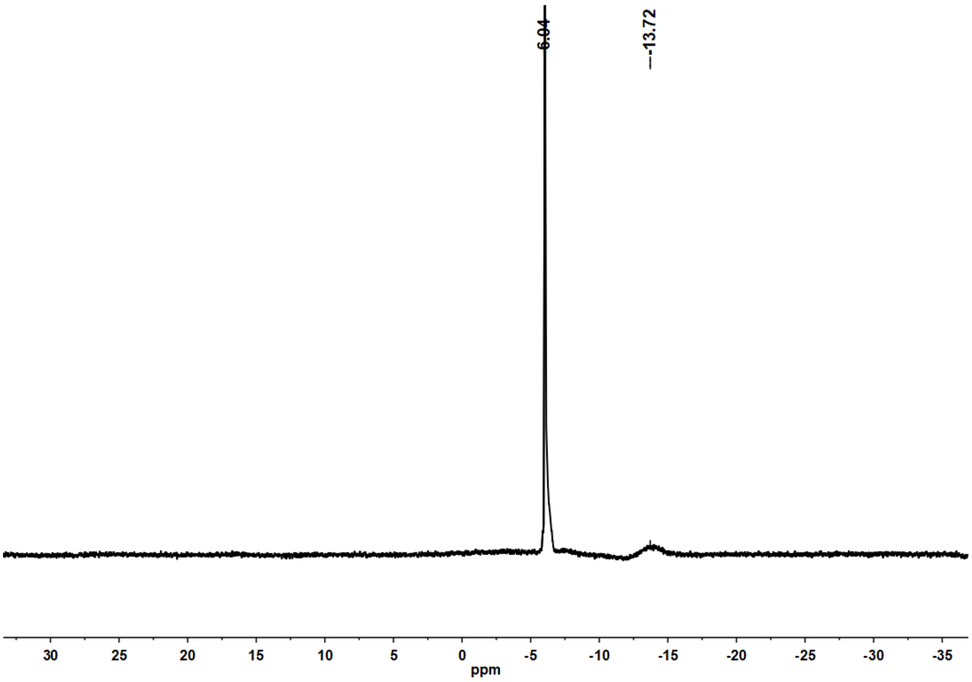

Figure S26. ^{11}B NMR spectrum of [**3H(PPh$_3$)**][BAr$_4^F$] in fluorobenzene.

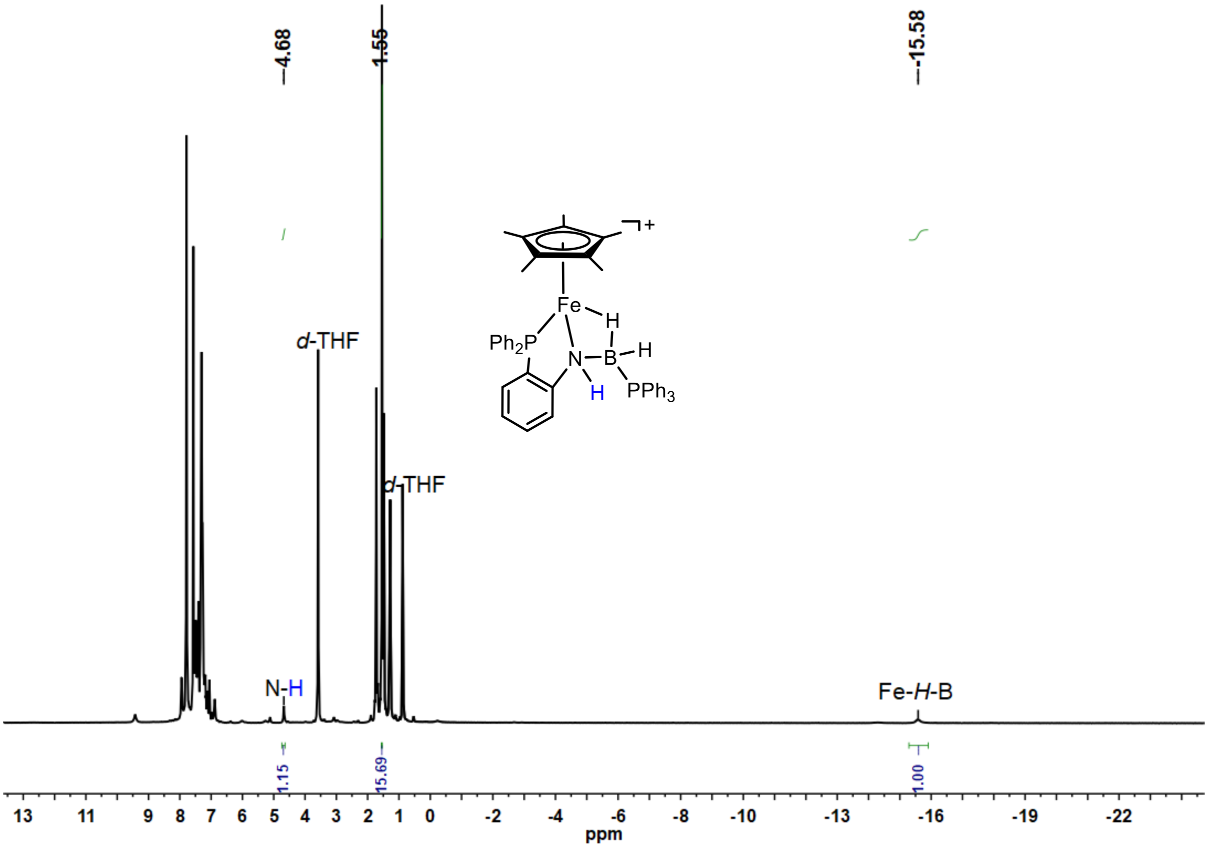

Figure S27. ^{1}H NMR spectrum of [**3H-PPh$_3$**][BAr$_4^F$] in d_8-THF.

7. Regenaration of Cp*Fe(1,2-$Ph_2PC_6H_4NH$)(η^1–BH_3) (3).

Protonation by $H(Et_2O)_2BAr_4^F$ and hydride transfer of HBcat • NEt_3. In a glovebox, Cp*Fe(1,2-$Ph_2PC_6H_4NH$)(η^1–BH_3) (**3**)(30 mg, 0.06 mmol) was dissolved in 5 mL of fluorobenzene in a vial and $H(Et_2O)_2BAr_4^F$ (63.1 mg, 0.06 mmol) was added to the solution. The solution was stirred for 30 min until [**3H**][BAr_4^F] was formed. In a seperate vial, catecholborane (6.7 µL, 0.06 mmol) and NEt_3 (8.7 µL, 0.06 mmol) were dissolved in 1 mL fluorobenzene and the mixture kept stirring for 10 min before it was added to the solution of [**3H**][BAr_4^F]. The reaction mixture was stirred at room temperature for 15 min, and in situ ^{31}P NMR and ^{11}B NMR were taken. The solvent was pumped off and the reaction residue was extracted with hexane. The extract was dried under vacuum and ^1H NMR spectrum was taken.

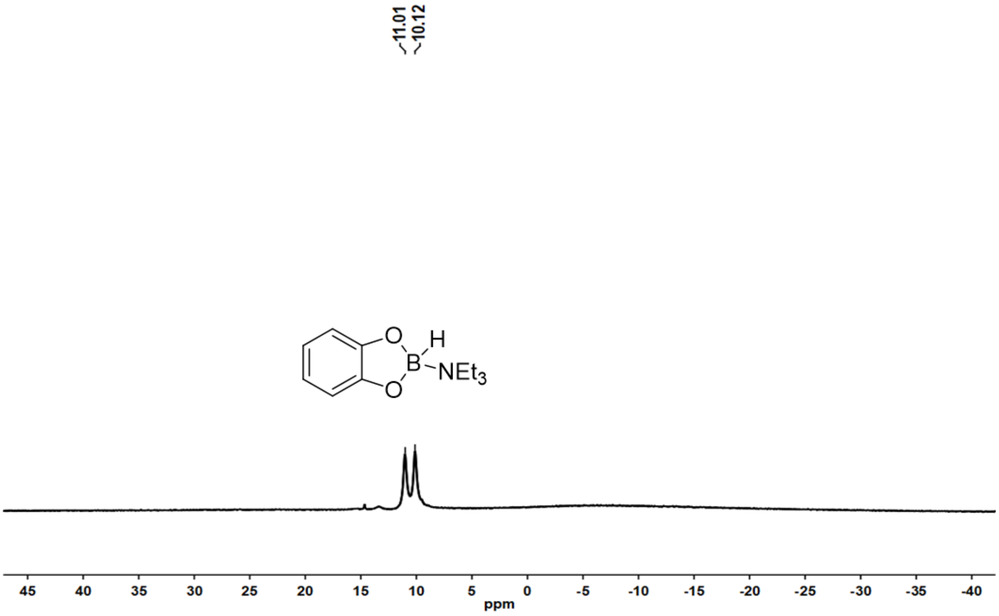

Figure S28. In situ ^{11}B NMR spectrum of catecholborane-NEt_3 adduct in fluorobenzene.

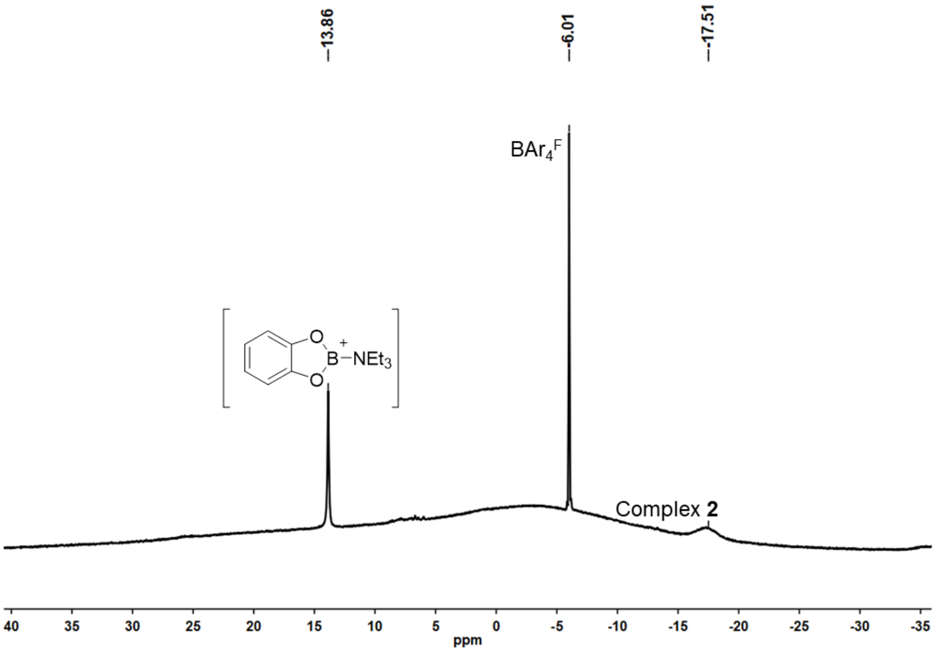

Figure S29. *In situ* ^{11}B NMR spectrum of the hydride transfer reaction in fluorobenzene.

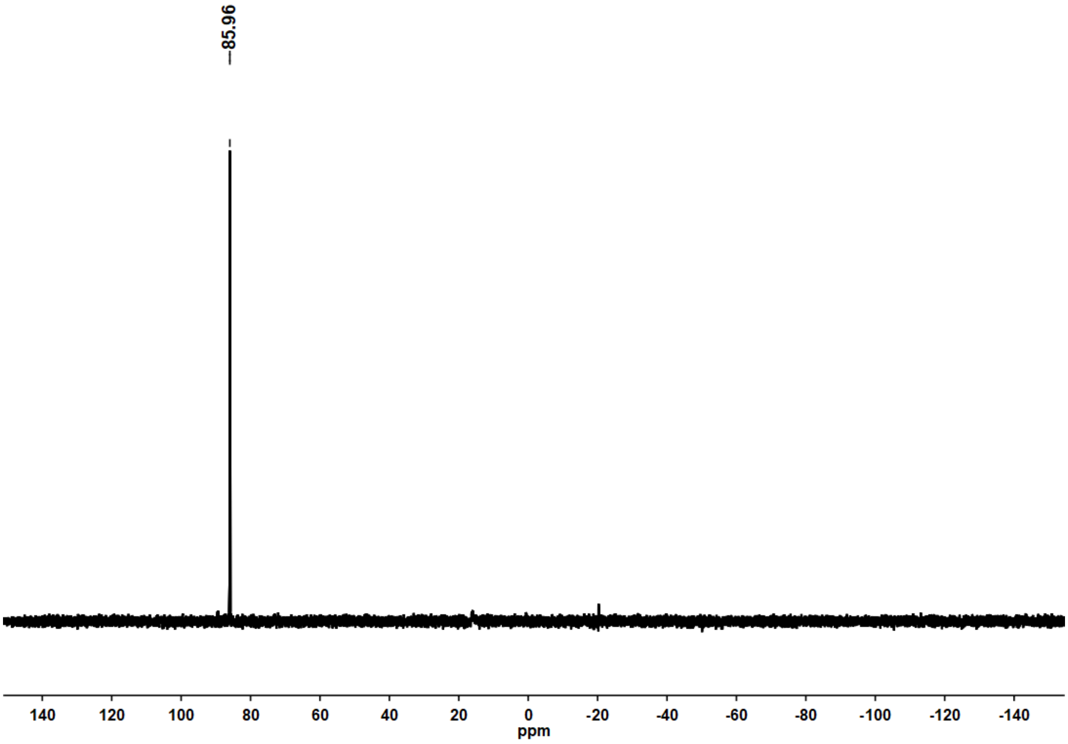

Figure S30. *In situ* ^{31}P NMR spectrum of the hydride transfer reaction in fluorobenzene.

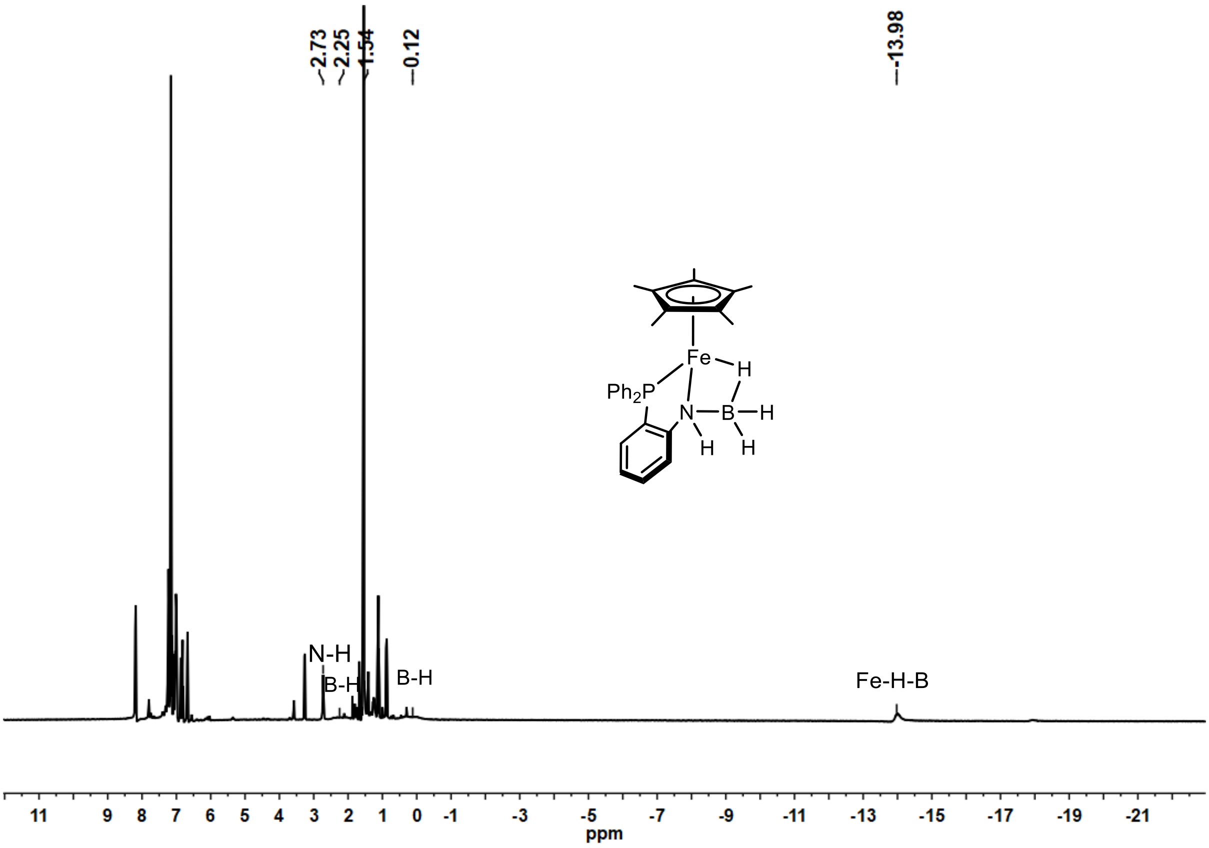

Figure S31. ^{1}H NMR spectrum of the hydride reaction extract in C_6D_6.

Other attempted hydride transfer reactions.

When freshly prepared [**3H**][BAr$_4^F$] was treated with 1-benzyl-1,4-dihydronicotinamide ($\Delta G_{\text{H-}}$ = 64.2 kcal/mol) or catecholborane-DABCO (1,4-diazabicyclo[2.2.2]octane) adduct ($\Delta G_{\text{H-}}$ = 60 kcal/mol), or Hantszch ester ($\Delta G_{\text{H-}}$ = 59 kcal/mol). No complex **2** was formed as monitored by ^{31}P NMR and ^{11}B NMR spectroscopy in 16 h.

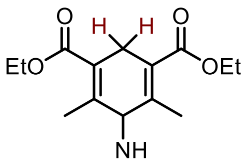

Hantszch ester used in the reaction

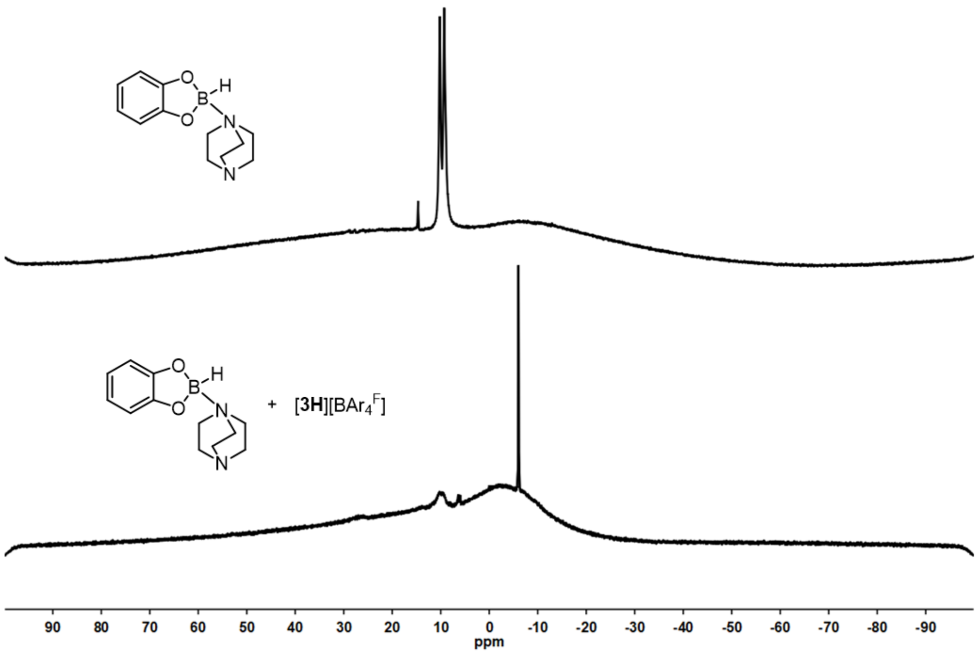

Figure S32. ^{11}B NMR of catecholborane-DABCO adduct and the reaction mixture of catecholborane-DABCO with [**3H**][BAr_4^F].

8. Dehydrogenation of ammonia borane catalyzed by complex 2 or 3.

Under argon, 5 mL of a THF solution of $H_3N \cdot BH_3$ (32 mg, 1.0 mmol) was placed into a 25 mL flask with a rubber plug. 1 mL of a THF solution of **2** or **3** (5 mg, 0.01 mmol) was injected to the reaction flask by syringe. Then, the flask was sealed with paraffin and the volume of the evolved hydrogen was monitored by GC-TCD with methane as the internal standard. A white suspension was formed during the reaction. The ^{11}B spectrum confirmed the presence of B-(cyclodiborazanyl)amine-borane (BCDB). The assignment of the signals agreed with the data reported by Berke et al.[4]

We monitored the reaction overnight by ^{31}P and ^{11}B NMR spectroscopy as shown below. The spectra were collected every 15 min. In ^{11}B NMR spectra, only the signals of **2** or **3** and H3N-BH3 or the product BCDB were observed in solution, and significant amount of precipitate formed during the reaction which is presumed to be some B-N polymers. No new signal was observed in ^{31}P NMR spectra (Figure S34 and S35)

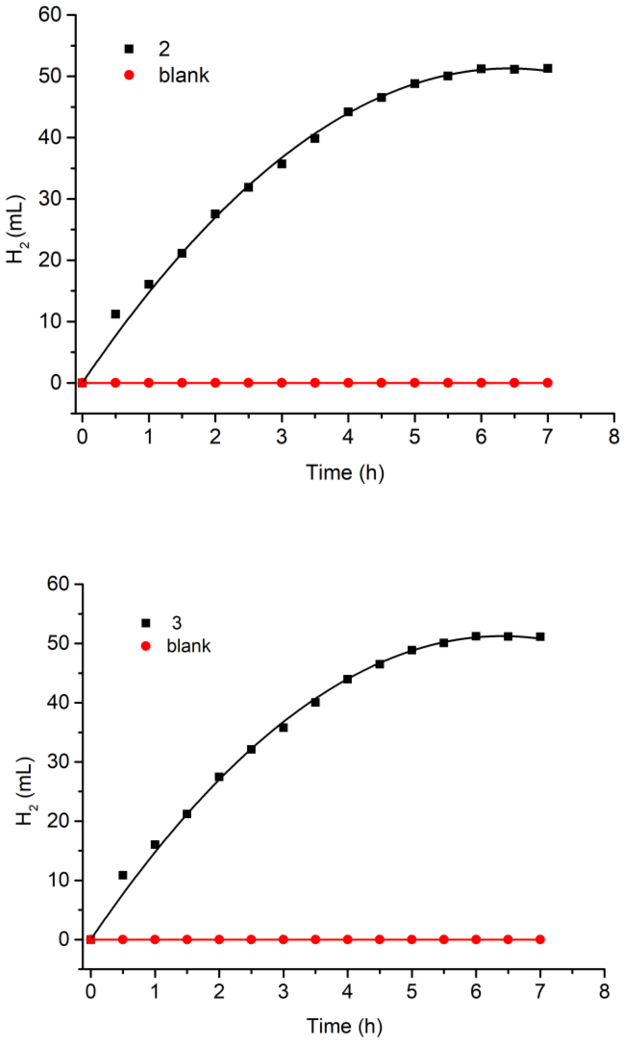

Figure S33. H_2 gas quantification of the catalytic dehydrogenation of $H_3N\cdot BH_3$ with **2** or **3** in THF at 298 K.

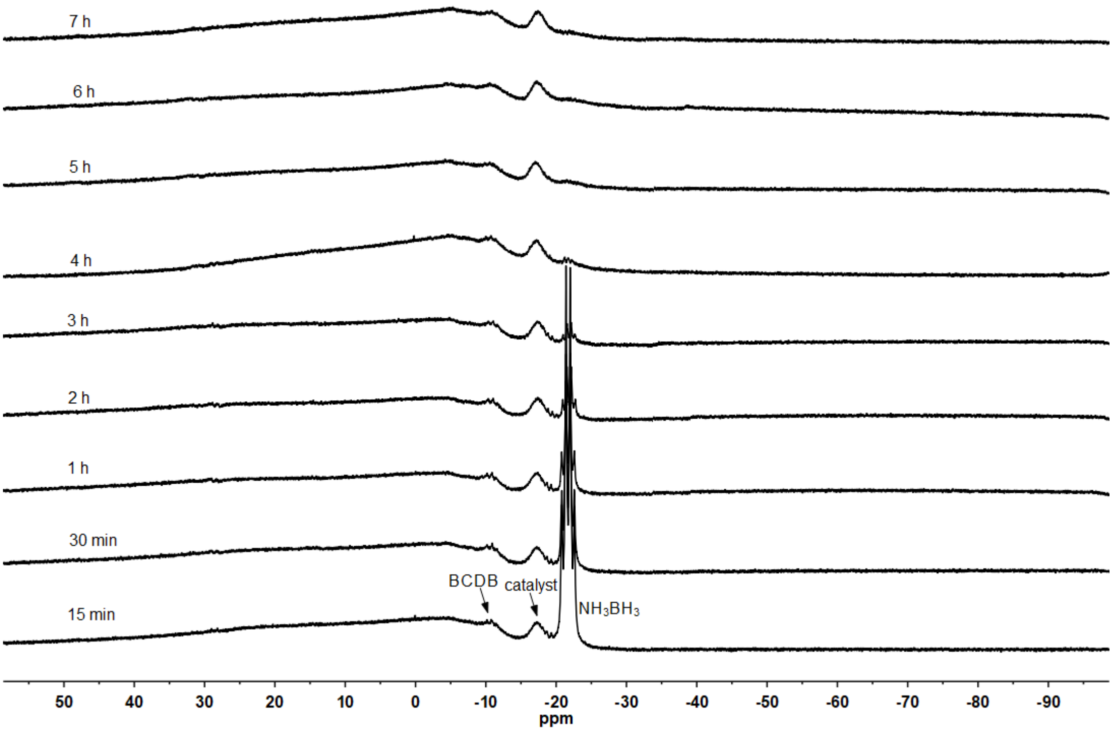

Figure S34. ^{11}B NMR spectra of the catalytic dehydrogenation of NH_3BH_3 with complex **2**. (BCDB = B-(cyclodoborazanyl)-aminoborohydride)

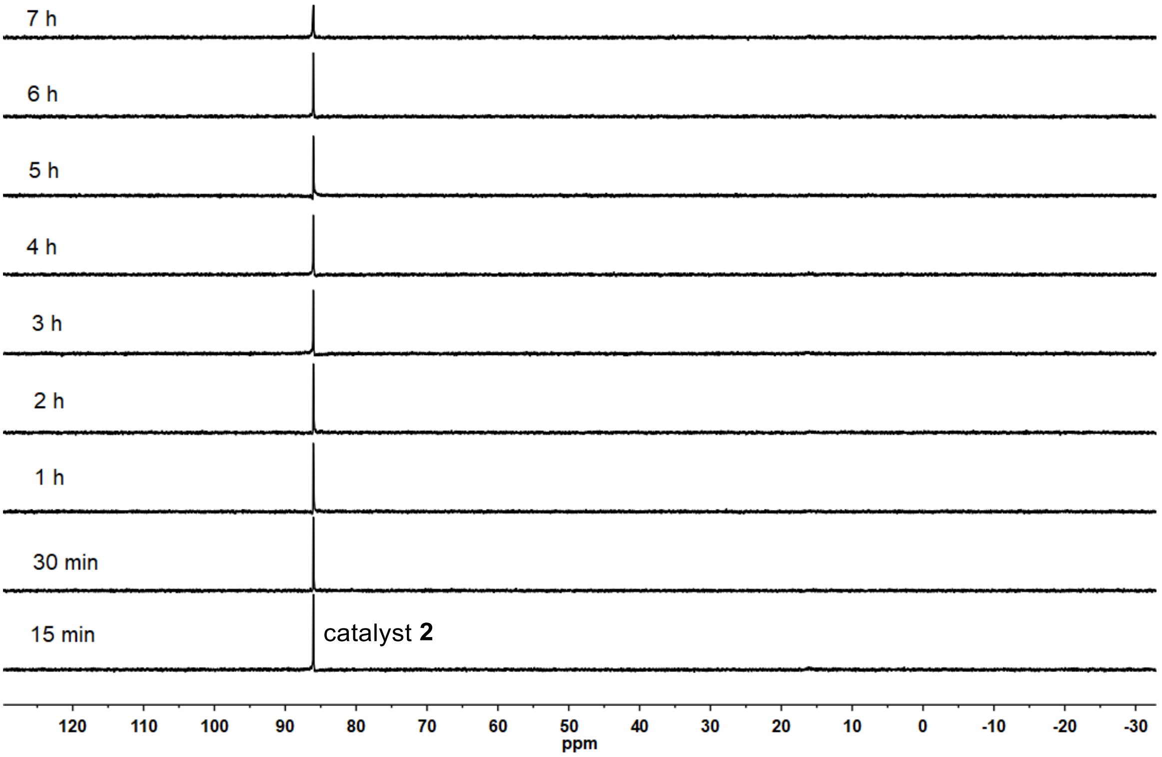

Figure S35. ^{31}P NMR spectra of the catalytic dehydrogenation of NH_3BH_3 with complex **2**.

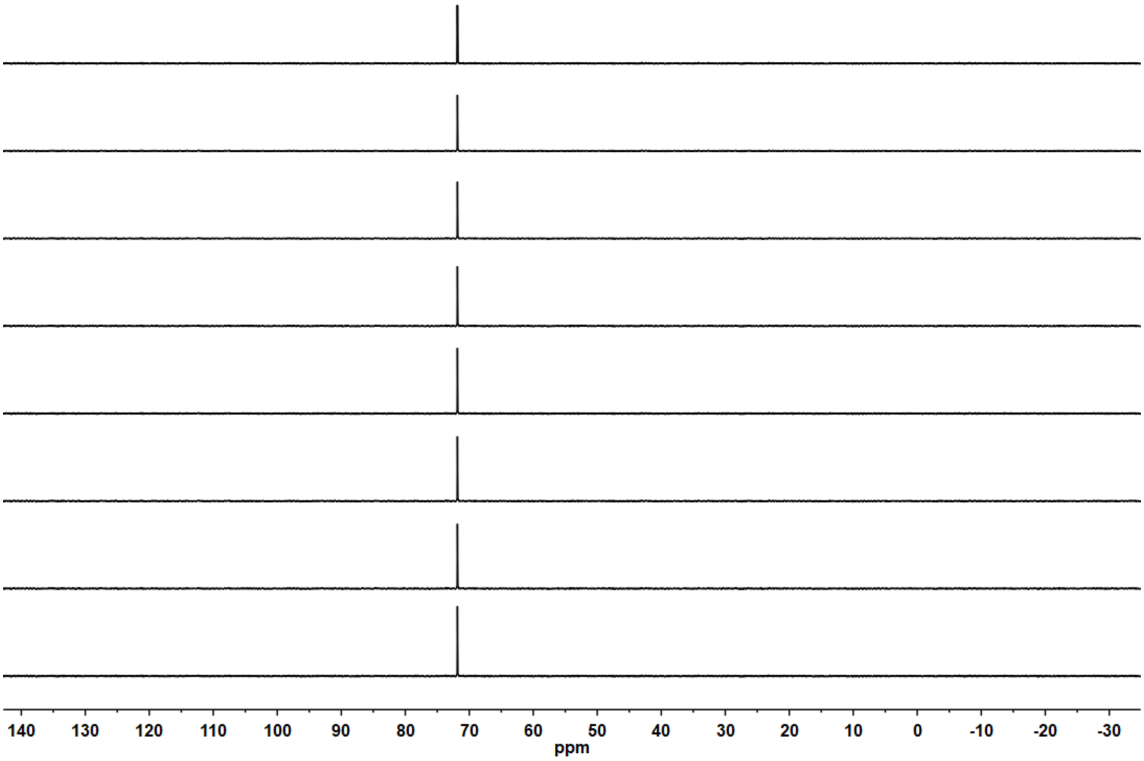

Figure S36. ^{31}P NMR spectra of the catalytic dehydrogenation of NH_3BH_3 with complex **3**.

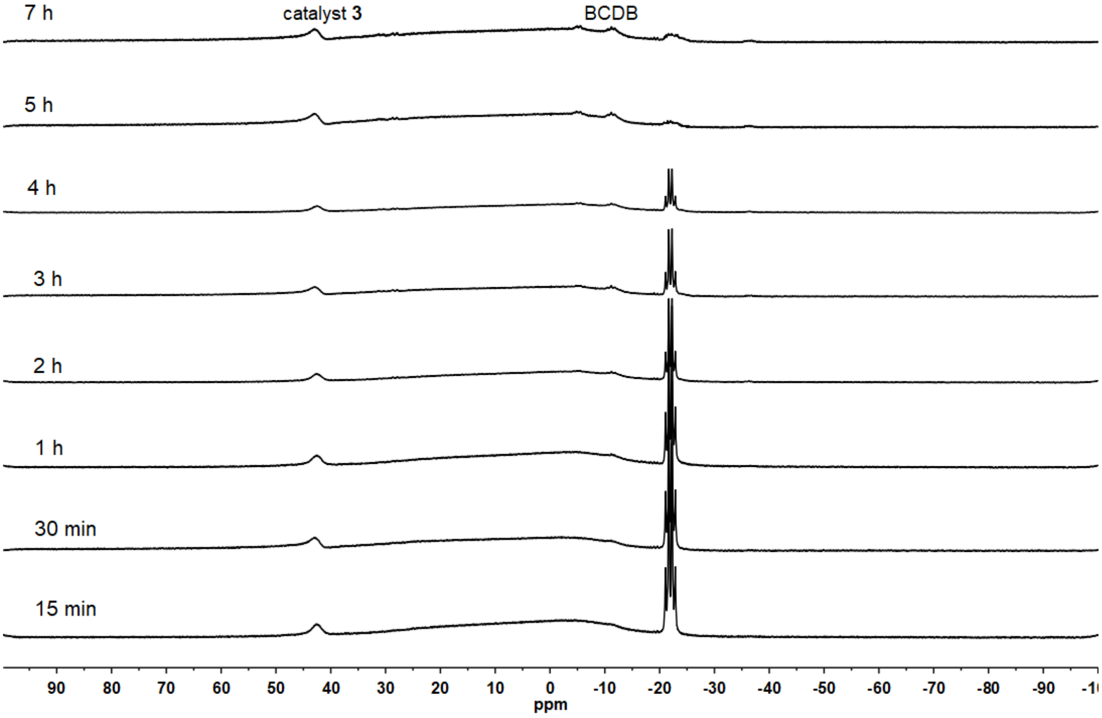

Figure S37. ^{11}B NMR spectra of the catalytic dehydrogenation of NH_3BH_3 with complex **3**. (BCDB = B-(cyclodoborazanyl)-aminoborohydride)

9. Transfer hydrogenation of quinoline to 1,2-dihydroquinolines catalyzed by complex 2 or 3.

Genearal procedure. In a glovebox, a scintillation vial (with a magnetic stir bar) was charged with quinoline (2 mmol), and $H_3N\cdot BH_3$ (2 mmol, 61.6 mg). The catalyst (10 mg, 0.02 mmol) and THF (2 ml) were added. The mixture was stirred at 25 ^{o}C for 6 h. After the indicated time, the reaction mixture was isolated by chromatography on silica gel eluting with EtOAc/petroleum ether to give the product.

Table S1. Catalytic transfer hydrogenation of quinolines by **2** or **3**

Entry	catalyst (loading)	R	Temperature	time (h)	yield (%)[a]
1	none	$-CH_3$	25 ^{o}C	8	0
2	none	$-CH_2COOCH_3$	25 ^{o}C	8	0
3	**2** (1 mol%)	$-CH_2COOCH_3$	25 ^{o}C	6	87 (96:4)[b]
4	**2** (1 mol%)	$-CH_2COOCH_3$	60 ^{o}C	6	88 (96:4)[b]
5	**2** (1 mol%)[c]	$-CH_2COOCH_3$	25 ^{o}C	6	85 (93:7)[b]
6	**3** (1 mol%)	$-CH_2COOCH_3$	25 ^{o}C	6	85 (98:2)[b]
7	**3** (1 mol%)	$-CH_2COOCH_3$	60 ^{o}C	6	86 (94:6)[b]
8	**3** (0.5 mol%)	$-CH_2COOCH_3$	25 ^{o}C	6	89 (92:8)[b]
9	**2** (1 mol%)	$-CH_3$	25 ^{o}C	6	93 (97:3)[b]
10	**3** (1 mol%)	$-CH_3$	25 ^{o}C	6	92 (95:5)[b]

[a] Isolated yield.

[b] Ratios in parentheses refer to product ratios of 1,2-DHQ and THQ determined by ^{1}H NMR spectroscopy.

[c] With 200 eqv. $H_3N\cdot BH_3$.

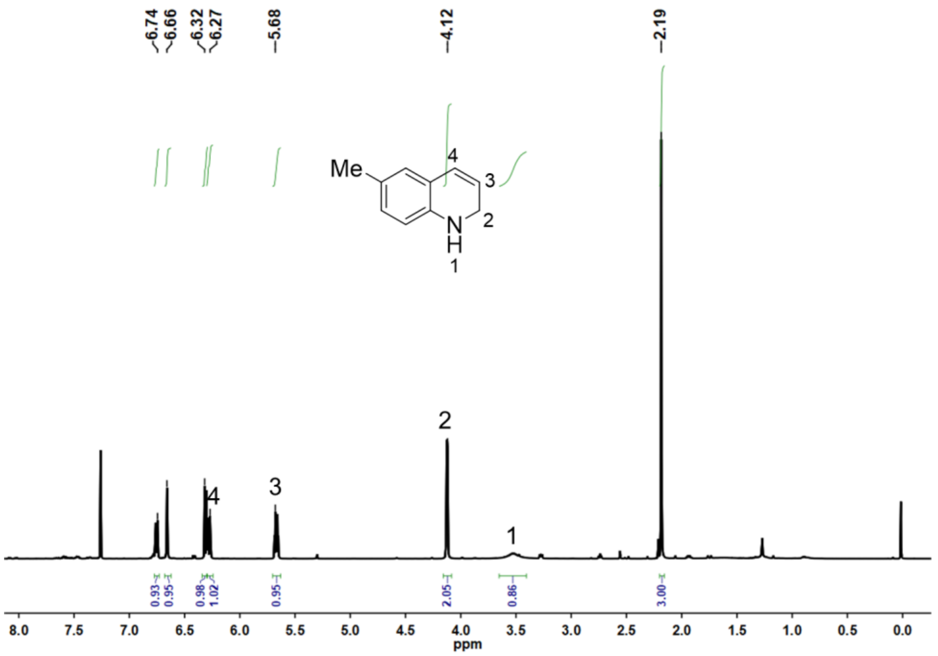

Figure S38. ^{1}H NMR spectrum of 1,2-dihydro-6-methyl-quinoline ($CDCl_3$).

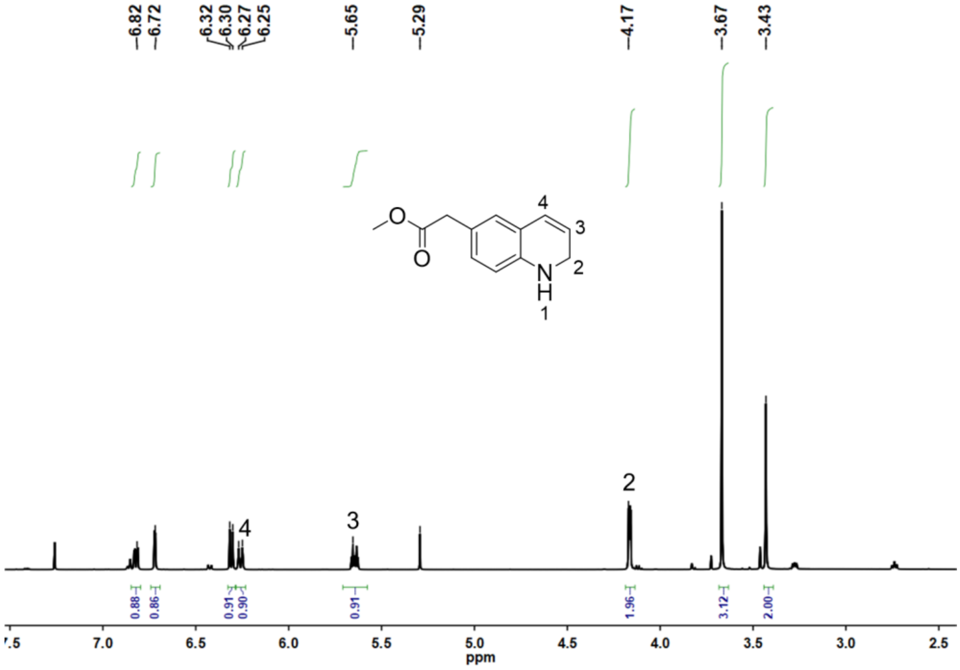

Figure S39. ^{1}H NMR spectrum of 1,2-dihydro-methyl-6-quinolineacetate ($CDCl_3$).

10. X-ray crystal structure determinations

Single crystals were coated with inert oil, placed under streaming nitrogen in a Bruker Apex II CCD diffractometer (Mo Kα radiation, λ = 0.71073 Å) and Rigaku Oxford Diffraction XtaLAB Synergy diffractometer equipped with a HyPix-6000HE area detector (Cu Kα radiation, λ = 1.54184 Å). The structures were solved using the charge-flipping algorithm, as implemented in the program *SUPERFLIP*[5] and refined by full-matrix least-squares techniques against F_o^2 using the SHELXL program[6] through the OLEX2 interface.[7] Hydrogen atoms bonded to carbon were placed at calculated positions and refined isotropically by using a riding model. Both structures were examined using the Addsym subroutine of PLATON[8] to ensure that no additional symmetry could be applied to the models. Crystallographic and experimental details of the structure determination are summarized in Table S2-S3. CCDC 2033258-2033262 contain the supplementary crystallographic data. These data are provided free of charge by The Cambridge Crystallographic Data Centre.

Table S2. Crystal data and structure refinement of complexes **1, 2** and **3**.

	1	**2**	**3**
Empirical formula	$C_{12}H_{22}BFeN$	$C_{28}H_{33}BFeNP$	$C_{168}H_{186}B_6Fe_6N_6P_6$
Formula weight	246.96	481.224	2875.00
Temperature / K	123(10)	100.01(10)	293(2)
Crystal system	monoclinic	monoclinic	monoclinic
Space group	$P2_1/c$	$P2_1/n$	$P2_1/c$
a / Å	12.5601(3)	10.668(4)	15.3228(2)
b / Å	7.39591(20)	10.792(4)	26.7339(3)
c / Å	14.8102(4)	21.922(8)	35.8973(4)
α / °	90	90	90
β /°	98.207(3)	92.119(3)	99.9300(10)
γ / °	90	90	90
Volume / Å^3	1361.68(6)	2522.1(15)	14484.6(3)
Z	4	4	4
ρ_{calc} / g cm^{-3}	1.205	1.267	1.318
μ / mm^{-1}	1.077	0.675	5.738
F(000)	528.0	1018.2	6048.0
2Θ range for data collection / °	3.272 to 50.152	5.36 to 55.18	5.856 to 153.29
Index ranges	$-13 \leq h \leq 15$, $-8 \leq k \leq 8$, $-15 \leq l \leq 17$	$-13 \leq h \leq 13$, $-14 \leq k \leq 13$, $-19 \leq l \leq 28$	$-18 \leq h \leq 19$, $-29 \leq k \leq 33$, $-45 \leq l \leq 41$
Reflections collected	6944	18179	81826

Independent reflections	2400 [R_{int} = 0.0438, R_{sigma} = 0.0456]	5800 [R_{int} = 0.0345, R_{sigma} = 0.0385]	28493 [R_{int} = 0.0626, R_{sigma} = 0.0622]
Data/restraints/ parameters	2400/150/254	5800/0/310	28493/0/1807
Goodness-of-fit on F^2	1.077	1.077	1.035
Final R indexes [I>2σ (I)]	R_1 = 0.0432 wR_2 = 0.1039	R_1 = 0.0370 wR_2 = 0.0883	R_1 = 0.0590 wR_2 = 0.1593
Final R indexes [all data]	R_1 = 0.0589 wR_2 = 0.1137	R_1 = 0.0554 wR_2 = 0.1009	R_1 = 0.1037 wR_2 = 0.1943
Largest diff. peak/hole / e Å^{-3}	0.43/-0.46	0.44/-0.42	0.79/-0.56

Table S3. Crystal data and structure refinement of complex [**3H**][BAr$_4^F$] and [**3H-PPh$_3$**][BAr$_4^F$].

	[**3H**][BAr$_4^F$]	[**3H-PPh$_3$**][BAr$_4^F$]
Empirical formula	$C_{68}H_{60}B_2F_{24}FeNO_2P$	$C_{81}H_{67}B_2F_{24}FeNP_2$
Formula weight	1487.61	1649.76
Temperature / K	173.00(10)	173.00(10)
Crystal system	triclinic	monoclinic
Space group	P-1	$P2_1/c$
a / Å	12.9415(3)	13.1206(2)
b / Å	14.6375(4)	16.6063(2)
c / Å	19.3031(5)	36.1078(5)
α / °	103.817(2)	90
β /°	92.601(2)	93.6090(10)
γ / °	92.604(2)	90
Volume / Å^3	3541.17(16)	7851.73(19)
Z	2	4
ρ_{calc} / g cm^{-3}	1.395	1.396
μ / mm^{-1}	2.872	2.817
F(000)	1516.0	3368.0
2Θ range for data collection / °	6.228 to 134.158	8.092 to 152.666
Index ranges	-15≤h≤12, -17≤k≤17, -23≤l≤23	-16≤h≤12, -20≤k≤19, -45≤l≤45
Reflections collected	35930	53180

Independent reflections	12459 [R_{int} = 0.0743, R_{sigma} = 0.0750]	15452 [R_{int} = 0.0489, R_{sigma} = 0.0486]
Data/restraints/parameters	12459/30/955	15452/150/1113
Goodness-of-fit on F^2	1.074	1.024
Final R indexes [I>2σ (I)]	R_1 = 0.0765, wR_2 = 0.2084	R_1 = 0.0806, wR_2 = 0.2199
Final R indexes [all data]	R_1 = 0.0924, wR_2 = 0.2379	R_1 = 0.0973, wR_2 = 0.2347
Largest diff. peak/hole / e $Å^{-3}$	0.92/-0.80	1.22/-0.63

11. Reference

(1) Gelman, D.; Jiang, L.; Buchwald, S. L. *Org Lett*. **2003**, *5*, 2315.

(2) (a) Walter, M. D.; White, P. S. *New J. Chem.* **2011,** *35*, 1842; (b) Zhang, F.; Jia, J.; Dong, S.; Wang, W.; Tung, C.-H. *Organometallics* **2016,** *35*, 1151.

(3) Gloaguen, Y.; Alcaraz, G. *J. Am. Chem. Soc.* **2011**, *133*, 17232.

(4) Yang, X.; Zhao, L.; Fox, T.; Wang, Z. X.; Berke, H. *Angew. Chem. Int. Ed.* **2010**, *49*, 2058.

(5) Palatinus, L.; Chapuis, G. *J. Appl. Crystallogr.* **2007,** *40*, 786.

(6) Sheldrick, G. M. *Acta Crystallogr. Sect. C* **2015,** *71*, 3.

(7) Dolomanov, O. V.; Bourhis, L. J.; Gildea, R. J.; Howard, J. A. K.; Puschmann, H. *J. Appl. Crystallogr.* **2009,** *42*, 339.

(8) Spek, A. L. *Acta Crystallogr. Sect. D* **2009,** *65*, 148.